NUREG/CR-6347
CNWRA 94-018

Multi-Phase Reactive Transport Theory

Manuscript Completed: May 1995
Date Published: July 1995

Prepared by
P. C. Lichtner

Southwest Research Institute
Center for Nuclear Waste Regulatory Analyses
6220 Culebra Road
San Antonio, TX 78228-0510

Prepared for
Division of Regulatory Applications
Office of Nuclear Regulatory Research
U.S. Nuclear Regulatory Commission
Washington, DC 20555-0001
NRC Job Code B6666

DISCLAIMER

ABSTRACT

Physicochemical processes in the near-field region of a high-level waste repository may involve a diverse set of phenomena including flow of liquid and gas, gaseous diffusion, and chemical reaction of the host rock with aqueous solutions at elevated temperatures. This report develops some of the formalism for describing simultaneous multicomponent solute and heat transport in a two-phase system for partially saturated porous media. Diffusion of gaseous species is described using the Dusty Gas Model which provides for simultaneous Knudsen and Fickian diffusion in addition to Darcy flow. A new form of the Dusty Gas Model equations is derived for binary diffusion which separates the total diffusive flux into segregative and nonsegregative components. Migration of a wetting front is analyzed using the quasi-stationary state approximation to the Richards' equation. Heat-pipe phenomena are investigated for both gravity- and capillary-driven reflux of liquid water. An expression for the burnout permeability is derived for a gravity-driven heat-pipe. Finally an estimate is given for the change in porosity and permeability due to mineral dissolution which could occur in the region of condensate formation in a heat-pipe.

CONTENTS

CONTENTS (Cont'd)

FIGURES

TABLES

ACKNOWLEDGMENTS

This report was prepared to document work performed by the Center for Nuclear Waste Regulatory Analyses (CNWRA) for the Nuclear Regulatory Commission (NRC) under Contract No. NRC-02-93-005. The activities reported here were performed on behalf of the NRC Office of Nuclear Regulatory Research, Division of Regulatory Applications. The report is an independent product of the CNWRA and does not necessarily reflect the views or regulatory position of the NRC.

The author wishes to express his gratitude to Mohan Seth for fruitful discussions during the course of this work. Thanks also go to B. Murphy, M. Seth, and H. Nguyen for their technical reviews, and B. Sagar for his programmatic review.

QUALITY OF DATA, ANALYSES, AND CODES

DATA: There are no CNWRA-generated data contained in this report. Sources for other data should be consulted for determining the level of quality for those data.

ANALYSES AND CODES: The V-TOUGH and PORFLOW codes are controlled under the CNWRA's Software Configuration Procedure. Other codes used in this work are not under software configuration management.

1 INTRODUCTION

1.1 REGULATORY NEED

An important step in assessing the isolation performance of the proposed high-level radioactive waste (HLW) repository at Yucca Mountain (YM), in southwest Nevada, is the estimation of the postclosure hydrothermal conditions in the near-field. Recent theoretical studies of near-field thermohydrologic processes in unsaturated tuff suggest that the dynamics of these hydrothermal conditions may determine: (i) the minimum time that the waste packages remain dry during boiling conditions and (ii) the rates of water reflux following return to sub-boiling conditions. These studies have led the U.S. Department of Energy (DOE) to consider a thermal-loading strategy (Buscheck and Nitao, 1993) that would have the advantages of:

- Extending the period of radionuclide containment in the engineered barrier system
- Delaying the period of controlled radionuclide release (and transport)
- Potentially reducing the sensitivity of total-system performance to hydrological variability

This thermal loading strategy is referred to as the "hot" or "extended-dry" repository concept. This strategy has a number of implications regarding the issue of compliance with the Nuclear Regulatory Commission (NRC) postclosure performance objectives of 10 CFR Part 60 (Nuclear Regulatory Commission, 1992) and U.S. Environmental Protection Agency (EPA) containment requirements of 40 CFR Part 191 (Environmental Protection Agency, 1992).

With respect to 10 CFR Part 60, the extended-dry concept has implications regarding the two performance objectives for the engineered barrier system (EBS) stated in 10 CFR 60.113(a)(1): (i) containment requirement for the HLW packages, and (ii) radionuclide release rate limit from the EBS. How well the EBS meets the first performance objective greatly depends on the hydrothermal conditions because the canister corrosion processes are a direct function of the presence of liquid water. Similarly, meeting the second performance objective will depend on the water flow rates past failed waste packages.

The extended-dry concept could potentially enhance the compliance margin with the current cumulative radionuclide release requirements set in Table 1-1 of 40 CFR Part 191. A favorable compliance margin may also exist even if the EPA standard is amended to include a numerical limit for dose-to-man. Such compliance margins may indeed provide a degree of robustness that reduces the sensitivity of total-system performance to spatial or temporal variations in the hydrological conditions in the far field.

While a number of aspects of the extended-dry concept appear beneficial to subsystem and total-system performance, detailed theoretical and experimental studies of this concept must be performed. Additional justification for studying near-field thermohydrologic conditions is derived from the fact that the NRC must be sufficiently knowledgeable about this strategy to conduct effective prelicensing activities, such as commenting on: (i) the DOE Total-System Performance Assessments (TSPAs) for YM, (ii) repository and EBS designs, and (iii) thermohydrologic field and laboratory experiments.

1.2 TECHNICAL OBJECTIVES

The central purpose of this report is to document a detailed review of the theoretical basis of currently available thermohydrologic computer codes that are being used in evaluations of the extended-dry concept. Specific topics reviewed include the mathematical models of heat transfer, two-phase fluid flow, and reactive transport. One aim is to derive the governing equations from the basic conservation laws of continuum mechanics, established constitutive relations, and thermodynamic equations of state. In addition, related topics are briefly discussed, such as: (i) the computational aspects of thermohydrologic codes, (ii) simplifying assumptions aimed at reducing the computational time, (iii) simple test cases considered useful for code verification and benchmarking, and (iv) methods of estimating porosity and permeability changes as a function of pore fluid chemistry. All these topics were reviewed with the intent of understanding the limitations and ranges of applicability of thermohydrologic codes to unsaturated tuff.

1.3 CONSIDERATIONS OF NEAR-FIELD PHENOMENA

The near-field region of a HLW storage facility is characterized by large perturbations in temperature, saturation, and chemical reactivity from ambient conditions. In the proposed unsaturated site at YM, temperatures can reach as high as 100 °C in the presence of liquid water at approximately 1 bar pressure. For a typical activation energy of 35 kJ $mole^{-1}$ for the kinetic rate constant, this activation energy implies an increase in the rate constant at 100 °C by approximately a factor of 20 from its value at 25 °C.

Of particular importance to the longevity of a HLW waste canister is the geochemistry of near-field groundwater that could potentially come in contact with the container. Depending on the composition of this fluid, the rate of corrosion and leaching of spent fuel could be greatly accelerated. Unique to the unsaturated repository design concept is the formation of salts caused by evaporation of water in the vicinity of waste canisters due to the elevated temperatures. The amount of water that can be evaporated depends not only on the initial saturation of the pore spaces in the rock adjacent to the canisters, but also on the flow of water toward the waste packages resulting from capillary forces and gravity driven flow.

The extent of salt deposition due to evaporation is a function of the ionic strength of the refluxing fluid as well as the length of time during which evaporation occurs. The greater the amount of salt deposited, the greater is the possibility for increased concentration of dissolved solids contained in fluid in the near-field region of the repository after it cools to levels below the boiling point of the salt solution. It is possible that the composition of the fluid in the near-field could reach levels of brine compositions for some period of time. Dilution occurs as the near-field becomes resaturated. Concentration of solutes in the fluid would decrease due to mixing of condensate water vapor with the ambient groundwater and mineral precipitation, and increase due to evaporation and mineral dissolution.

Formation of salts, such as halite (NaCl), will depend on the amount of chloride available since it is not contained in the host rock minerals. Because of the high ionic strength solutions that can be produced by evaporation, it is necessary to take into account activity coefficient corrections on the concentrations of the solvent and solute species. The deposition of salts is expected to be a complicated function of repository geometry and the presence or absence of fractures. Deposition of salt will raise the

boiling point (lower vapor pressure) of the salt solution and could lead to wetting of the repository earlier than suggested by the DOE analyses of the extended-dry concept.

At present, it is within the realm of powerful, modern computer workstations to perform the necessary calculations to investigate the effects of liquid evaporation and condensation on the possibility of brine formation in the near-field region of a HLW repository. Such calculations involve two-phase fluid transport in a partially saturated porous medium coupled to multicomponent solute transport and fluid/rock interaction.

1.4 REPORT ORGANIZATION

The work begins with definitions of field variables in various representations of concentration variables followed by a derivation of the conservation equations for mass and heat including chemical reactions involving mineral precipitation/dissolution, aqueous complexing reactions, gaseous reactions, and ion-exchange. Attention is given to the water vapor-liquid phase transition. The next chapter presents an outline of the dusty gas model for describing gaseous diffusion in a porous medium when the molecular mean free path of the gas is on the order of or greater than the pore size dimension. Several relations for the segregative and nonsegregative components of the diffusive flux are derived. This discussion is restricted, however, to isothermal systems. The following section discusses the Richards' equation, which describes how transport in a partially saturated porous medium is solved for both transient and quasi-stationary state conditions using an adaptive gridding technique. The results are compared for a wetting front penetrating into the YM tuff matrix. Two examples of one-dimensional (1D) heat pipes are considered with both gravity- and capillary-driven mechanisms of liquid reflux. Finally, estimates are given for changes in porosity and permeability under far from equilibrium conditions for dissolution of a tuffaceous host rock. Precipitation of secondary minerals is not considered, however.

2 MULTICOMPONENT HEAT AND MASS TRANSPORT IN PARTIALLY SATURATED POROUS MEDIA

This section provides a review of the basic equations used in numerical modeling codes involving heat and multiphase fluid transport. Emphasis is placed on calculating rates of evaporation and condensation of water vapor, which are important to describing the near-field environment of a HLW repository under unsaturated conditions, fluid/rock interaction represented by mineral precipitation/dissolution reactions, and ion-exchange.

2.1 DEFINITION OF FIELD VARIABLES

The quantitative description of the transport of fluids and their interaction with rocks is based on a mathematical representation of the real physical system referred to as a continuum. In this theory, the actual discrete physical system, consisting of aggregates of minerals, interstitial pore spaces, and fractures, is replaced by a set of interacting continua coexisting at each point in space. Each continuum represents a different phase of the system corresponding to a fluid phase (liquid or gas), or solid. In the continuum representation, the physical variables describing the system, which are discontinuous on a microscopic scale as a consequence of the granular nature of rocks, are replaced by functions that are continuous on a macroscopic scale, that is the scale of the representative elemental volume (REV). Such variables include the porosity, temperature, pressure, aqueous concentrations of solute species, and mineral modal abundances and composition. These functions defined at each point in space and time are referred to mathematically as fields. Thus, for example, the temperature T is represented by the function $T(\mathbf{r}, t)$ where the vector $\mathbf{r}$ refers to a point in the rock with coordinates (x, y, z). The value of the temperature at the point $\mathbf{r}$ is obtained by averaging the temperature over a REV centered at $\mathbf{r}$. Similarly, the porosity, mineral modal abundance, and aqueous concentration are represented by the fields $\phi(\mathbf{r},t)$, $\phi_m(\mathbf{r},t)$, and $C_i(\mathbf{r},t)$, respectively.

A rock consisting of an ensemble of mineral grains and pore spaces is referred to as a porous medium. The total porosity, ϕ, of the porous medium is defined as the fraction of volume of the rock made up of pore space or voids. (The total porosity may be connected or disconnected, which would consist of isolated pores.) To determine the porosity quantitatively, it is necessary to consider a representative sample of rock that locally typifies the average characteristics of the mineral grain sizes and pore spaces. This volume is referred to as representative elemental volume. A REV may be the size of a hand sample collected by a geologist in the field, but it may also be much smaller, perhaps on the order of tens of mineral grains or larger. For rocks exhibiting patterns such as reaction halos surrounding fractures, care must be taken to choose the size of the REV smaller than the size of the structure being observed. The REV should not be too small, however, since then it no longer provides an average property of the rock. The REV is large compared to the pore volume, but small compared to the characteristic length scale over which quantities of interest change. These items of interest include temperature, pressure, solute concentration, mineral modal abundance, and other field variables that describe the system. The essential feature of a REV is that it characterizes the properties of the system locally. Covering the entire system with a connected set of REVs provides a global description of the system. There is no guarantee that a single set of REVs is sufficient to characterize a rock. This insufficiency is especially true of fractured rocks for which a primary and secondary porosity can be defined. For such rocks, at least two sets of REVs are needed, one for the fracture system and the other for the rock matrix. More generally a hierarchial porous medium may require many sets of REVs to be

properly characterized (multiple continua). It is important to realize that a continuum theory can provide only a macroscopic description of the properties of rocks and not a microscopic description. This is not to say that microscopic properties are not important. In some cases, it is the microscopic properties averaged over a REV that provide values for the macroscopic properties. However, usually such averages are too difficult to perform mathematically, and we must let nature carry out the average for us. We may therefore attempt to measure directly the macroscopic properties of a rock, such as its porosity, thereby providing a phenomenological or empirical description. Even if it is not feasible to predict the values of the various parameters entering a continuum theory of fluid/rock interaction from fundamental principles, a phenomenological description can provide a first attempt to model such systems.

Mass conservation equations for energy and mass are referenced to a representative elemental volume of a porous medium. The volume of the REV, denoted by V_{REV} or simply V, is equal to the sum of solid volume V_s and void, or pore, volume V_p:

$$V_{\mathrm{REV}} = V_s + V_p \,. \tag{2-1}$$

The solid volume is assumed to consist of an aggregate of minerals, each with volume V_m. Likewise, the pore or void space is occupied by a number of fluid phases, each with volume V_f. The pore and solid volumes may be further expressed in terms of the individual phases which occupy them:

$$V_p = \sum_f V_f \,, \tag{2-2}$$

and

$$V_s = \sum_m V_m \,, \tag{2-3}$$

where the subscripts f and m denote the fth fluid phase and mth mineral, respectively. The total porosity ϕ of the porous medium is defined as the ratio of the pore volume to the REV volume

$$\phi = \frac{V_p}{V} \,. \tag{2-4}$$

The saturation S_f, giving the fraction of the pore volume occupied by fluid phase f, is defined by

$$S_f = \frac{V_f}{V_p} \,. \tag{2-5}$$

It follows from the definition of S_f that

$$\sum_f S_f = 1 \ . \tag{2-6}$$

2.1.1 Composition of a Phase

The composition of an arbitrary phase, π, is specified once the mole numbers n_i^π of each of the constituent species is known within each REV. The phase π may correspond to the aqueous solution, gas phase, or an individual mineral. Equivalently, the masses m_i^π may be substituted for the mole numbers. A number of different concentration scales can be used to describe the composition of a phase. The concentration (molarity) of the ith species in the π th fluid phase is given in the mole-representation by

$$c_i^\pi = \frac{n_i^\pi}{V_\pi}, \tag{2-7}$$

and in the mass-representation by

$$\rho_i^\pi = \frac{m_i^\pi}{V_\pi}. \tag{2-8}$$

The two concentration scales are related by the gram formula weight M_i of the ith species:

$$\rho_i^\pi = M_i c_i^\pi. \tag{2-9}$$

Additional variables used to describe a multicomponent system are mass and mole fraction. The mass fraction w_i^π is defined by

$$w_i^\pi = \frac{m_i^\pi}{m_\pi}, \tag{2-10}$$

with

$$m_\pi = \sum_i m_i^\pi \ . \tag{2-11}$$

The mole fraction x_i^π is defined by

$$x_i^\pi = \frac{n_i^\pi}{n_\pi}, \tag{2-12}$$

with

$$n_\pi = \sum_i n_i^\pi. \tag{2-13}$$

The mole and mass fractions satisfy the relation

$$\sum_i x_i^\pi = \sum_i w_i^\pi = 1, \tag{2-14}$$

and, therefore, they are not independent variables. Consequently, mass and mole fractions do not provide in themselves a complete description of the phase composition. By making use of the relation between mass m_i^π and mole number n_i^π

$$n_i^\pi = \frac{m_i^\pi}{M_i}, \tag{2-15}$$

the mole fraction x_i^π and mass (weight) fraction w_i^π can be related by the expressions:

$$w_i^\pi = \frac{m_i^\pi}{\sum_l m_l^\pi} = \frac{M_i n_i^\pi}{\sum_l M_l n_l^\pi} = \frac{M_i x_i^\pi}{\sum_l M_l x_l^\pi}, \tag{2-16}$$

and

$$x_i^\pi = \frac{n_i^\pi}{\sum_l n_l^\pi} = \frac{M_i^{-1} m_i^\pi}{\sum_l M_l^{-1} m_l^\pi} = \frac{M_i^{-1} w_i^\pi}{\sum_l M_l^{-1} w_l^\pi}. \tag{2-17}$$

The intrinsic density of each phase can be expressed alternatively as

$$\rho_\pi^0 = \frac{m_\pi}{V_\pi}, \tag{2-18}$$

and

$$c_{\pi}^{0} = \frac{n_{\pi}}{V_{\pi}}, \tag{2-19}$$

in the mass and mole-number representations, respectively.

2.1.1.1 Molality

A measure of solute concentration of special importance for describing aqueous solutions is the molality scale. Molality m_i^l, moles of solute per kilogram of solvent, can be represented as

$$\mathrm{m}_i^l = \frac{n_i^l}{m_w^l} = \frac{x_i^l}{M_w x_w^l}, \tag{2-20}$$

where the subscript w denotes the solvent, or, alternatively, in terms of weight fractions as

$$\mathrm{m}_i^l = \frac{w_i^l}{M_i w_w^l}. \tag{2-21}$$

As the amount of solvent decreases for a fixed number of moles of solute, the molality increases, eventually approaching infinity as all solvent evaporates. Such a process is caused by evaporation, for example, and can lead to extremely saline solutions. For a sufficiently dilute solution, $x_i^l << x_w^l \simeq 1$ and

$$\mathrm{m}_i^l \simeq \frac{x_i^l}{M_w} \simeq \frac{w_i^l}{M_i}. \tag{2-22}$$

The molality and molarity concentration scales are related by the expression

$$c_i^l = \rho_l w_w^l \mathrm{m}_i^l. \tag{2-23}$$

For a dilute solution

$$c_i^l = \rho_l \mathrm{m}_i^l. \tag{2-24}$$

The molarity concentration scale c_i^l is related to the mole fraction scale by the equation

$$c_i^l = \rho_l^0 \frac{n_i^l}{\sum_{i'} M_{i'} n_{i'}^l} = \rho_l^0 \frac{x_i^l}{\sum_{i'} M_{i'} x_{i'}^l}, \tag{2-25}$$

obtained by using the relation

$$\rho_l^0 V_l = \sum_i M_i n_i^l \ . \tag{2-26}$$

For dilute aqueous solutions this expression reduces to

$$c_i^l = \rho_l^0 \frac{x_i^l}{M_w} \ . \tag{2-27}$$

Summing Eq. (2-25) over i yields

$$c_l^0 = \frac{\rho_l^0}{\sum_i M_i x_i} \ , \tag{2-28}$$

providing a relation between molar and mass density.

2.1.2 Solid Phase

In order to describe the characteristics of a porous medium quantitatively, it is necessary to introduce a set of descriptive variables specifying the amount and composition of each mineral present in a REV. There are a number of possibilities for introducing these variables, each with its own advantages and disadvantages. In the following volume fraction, mass fraction and mass density are discussed and their relation to each other derived. The variables $\{\phi_m\}$, $\{x_m, \phi\}$, and $\{\rho_m, \phi\}$ defined below, provide equivalent descriptions of the solid portion of the porous medium.

2.1.2.1 Volume Fraction

The amount or concentration of a particular solid can be represented by the mineral volume fraction ϕ_m, defined by

$$\phi_m = \frac{V_m}{V} . \tag{2-29}$$

Summing over all minerals in the REV yields the equation

$$\sum_m \phi_m = \frac{1}{V} \sum_m V_m = \frac{V_s}{V} = 1 - \phi \ . \tag{2-30}$$

relating the mineral volume fractions to the porosity. Thus, the total porosity and mineral volume fractions are not independent. It is sufficient to know the mineral volume fractions from which the porosity can be computed. Consequently, volume fractions are a preferred set of variables to describe the composition of a porous medium. It must be kept in mind, however, that the porosity defined above is the total porosity of the rock which may be different from the connected flow porosity.

2.1.2.2 Mass Fraction

The relationship between mass fraction and volume fraction can be obtained as follows. The mass m_m of the mth mineral is related to the volume V_m occupied by the mineral according to

$$m_m = M_m \bar{V}_m^{-1} V_m \,, \tag{2-31}$$

where M_m denotes the formula weight of the mth mineral and $\bar{V}_m$ denotes the corresponding molar volume. The molar volume is related to the intrinsic mineral density ρ_m^0 by the expression

$$\rho_m^0 = \frac{m_m}{V_m} = M_m \bar{V}_m^{-1}. \tag{2-32}$$

According to the definition of mass fraction, it follows that

$$w_m = \frac{M_m \bar{V}_m^{-1} V_m}{\sum_{m'} M_{m'} \bar{V}_{m'}^{-1} V_{m'}} \,. \tag{2-33}$$

Dividing numerator and denominator of this relation by the volume of the REV, yields the desired relation in terms of volume fractions:

$$w_m = \frac{M_m \bar{V}_m^{-1} \phi_m}{\sum_{m'} M_{m'} \bar{V}_{m'}^{-1} \phi_{m'}} \,. \tag{2-34}$$

The mass fraction w_m can be expressed in terms of the intrinsic mineral density according to

$$w_m = \frac{\rho_m^0 \phi_m}{\sum_{m'} \rho_{m'}^0 \phi_{m'}} \,. \tag{2-35}$$

The inverse relation is given by

$$\phi_m = (1 - \phi) \frac{\left(\rho_m^0\right)^{-1} w_m}{\sum_{m'} \left(\rho_{m'}^0\right)^{-1} w_{m'}}, \tag{2-36}$$

which involves the porosity of the porous medium. The quantity in the denominator in the equation for w_m is equal to the bulk rock density ρ_s^{bulk}:

$$\sum_m \rho_m^0 \phi_m = \frac{m_s}{V} = \rho_s^{\text{bulk}} \,, \tag{2-37}$$

where m_s denotes the total mass of the rock contained in the REV. The bulk density is related to the intrinsic rock density ρ_s and porosity by the equation

$$\rho_s^{\text{bulk}} = \frac{m_s}{V} = \frac{m_s}{V_s}\frac{V_s}{V} = \rho_s(1-\phi) , \tag{2-38}$$

where the intrinsic rock density is defined by

$$\rho_s = \frac{m_s}{V_s} . \tag{2-39}$$

The total porosity is related to the ratio of the bulk and intrinsic rock density by the expression

$$\phi = 1 - \frac{\rho_s^{\text{bulk}}}{\rho_s} . \tag{2-40}$$

From this relation it is possible to determine the total rock porosity from knowledge of both the bulk density and intrinsic density of the rock.

With these relations, the mass fraction can be expressed in the equivalent form

$$w_m = \frac{\rho_m^0 \phi_m}{(1-\phi)\rho_s} . \tag{2-41}$$

Dividing both sides of Eq. (2-41) by ρ_m^0 and summing over m yields an equivalent expression for the rock density in terms of mass fractions given by

$$\sum_m \left(\rho_m^0\right)^{-1} w_m = \rho_s^{-1} . \tag{2-42}$$

As pointed out above, knowing only the mass fractions w_m is insufficient information to provide a complete determination of the mineral volume fractions and thus to characterize the solid composition of the porous medium completely. In addition, it is necessary to know the porosity of the porous medium.

The volume fraction can be expressed in terms of the mass fraction and porosity by the inverse relation

$$\phi_m = \frac{\rho_s}{\rho_m^0}(1 - \phi)w_m , \tag{2-43}$$

or in terms of the bulk density by the equation

$$\phi_m = \frac{\rho_s^{bulk}}{\rho_m^0} w_m \ . \tag{2-44}$$

For the situation in which the intrinsic densities ρ_m^0 are approximately independent of m, it follows that

$$w_m \propto \frac{\phi_m}{1 - \phi} . \tag{2-45}$$

Thus, in this approximation the mass fraction can be directly computed from the mineral volume fractions and porosity. The condition $\rho_m^0 \propto \rho$ independent of m implies that ρ is equal to the density of the rock according to

$$\rho_m^0 \propto \rho = \rho_s \ , \tag{2-46}$$

as follows from Eq. (2-41).

2.1.2.3 Mass Density of Solids

Mass density, defined as the mass relative to the total solid volume, is related to mass fraction by

$$\rho_m = \frac{m_m}{V_s} = \frac{m_m}{m_s} \frac{m_s}{V_s} = w_m \rho_s \ . \tag{2-47}$$

The intrinsic rock density is equal to the sum of the individual mineral mass densities according to the equation

$$\rho_s = \sum_m \rho_m \ . \tag{2-48}$$

The volume fraction and mass density are related by the intrinsic density ρ_m^0 and the total porosity according to the expression

$$\rho_m = \frac{\rho_m^0 \phi_m}{1 - \phi} \ . \tag{2-49}$$

The volume fraction is obtained from the mass density by the inverse relation

$$\phi_m = (1 - \phi)\left(\rho_m^0\right)^{-1}\rho_m \ . \tag{2-50}$$

2.1.3 Gas Phase

It is generally possible to assume ideal gas behavior for the gas phase at low (e.g., atmospheric) pressures, simplifying the calculations compared to real gases. For a mixture of ideal gases with constituent mole-numbers n_1, n_2,... at temperature T and pressure p, the equation of state is represented by the relation

$$V(T,p;n_1,n_2,...,n_c) = \frac{RT}{p}\sum_i n_i = \sum_i V_i \ , \tag{2-51}$$

with

$$V_i = n_i\bar{V}_i = \frac{n_i RT}{p} \ . \tag{2-52}$$

The partial molar volume of an ideal gas is thus given by

$$\bar{V}_i = \frac{RT}{p} \ , \tag{2-53}$$

and is independent of the particular species i. Alternatively, the equation of state of an ideal gas can be expressed as:

$$pV = NRT, \tag{2-54}$$

where

$$N = \sum_i n_i \ . \tag{2-55}$$

From this expression, the mole density of the gas is given by

$$c = \frac{N}{V} = \frac{p}{RT} \ . \tag{2-56}$$

For an ideal gas, the mass density can be expressed, alternatively, in terms of mole or weight fractions as

$$\rho = \frac{p}{RT}\sum_i M_i x_i = \frac{p}{RT}\frac{1}{\sum_l w_l M_l^{-1}} \ . \tag{2-57}$$

It follows that the pure mass density ρ_i^0 is equal to

$$\rho_i^0 = \frac{m_i}{V_i} = \frac{p}{RT}\frac{m_i}{n_i} = \frac{pM_i}{RT} . \tag{2-58}$$

For an ideal gas, the volume fraction ϕ_i is equal to the mole fraction

$$\phi_i = \frac{V_i}{V} = \frac{n_i RT}{pV} = \frac{n_i}{N} = x_i . \tag{2-59}$$

Consequently, the density of the mixture can be expressed as

$$\rho = \sum_i x_i \rho_i^0 = \sum_i f_i w_i \rho_i^0 , \tag{2-60}$$

where the weight factor f_i is equal to

$$f_i = \frac{1}{M_i \sum_l w_l M_l^{-1}} . \tag{2-61}$$

This expression was given incorrectly by Nitao (1988), who omitted the weight factor f_i. However, examination of the V-TOUGH source code revealed that the correct equation, Eq. (2-61), is used in the computer program.

Introducing the partial pressure p_i by the equation

$$p_i V = n_i RT , \tag{2-62}$$

the total pressure of an ideal gas mixture is equal to

$$p = \sum_i p_i . \tag{2-63}$$

Accordingly, the mole fraction can be expressed in terms of partial pressures as

$$x_i = \frac{n_i}{N} = \frac{p_i}{p} , \tag{2-64}$$

and

$$w_i = \frac{M_i p_i}{\sum_l M_l p_l} . \tag{2-65}$$

The density of an ideal gas mixture can be expressed in terms of the partial pressures according to the equation

$$\rho = \frac{1}{RT}\sum_i M_i p_i \ . \tag{2-66}$$

2.2 CONSERVATION EQUATIONS IN A MULTIPHASE SYSTEM

Consider a system consisting of a number of fluid phases denoted by π and chemical constituents denoted by the subscript i. Each fluid phase is represented by a equation of state V_π of the form:

$$V_\pi = V_\pi\left(T,p;n_1^\pi,n_2^\pi,...,n_c^\pi\right) , \tag{2-67}$$

in terms of mole-numbers, or equivalently

$$V_\pi = V_\pi\left(T,p;m_1^\pi,m_2^\pi,...,m_c^\pi\right), \tag{2-68}$$

in terms of masses of the individual constituents.

2.2.1 Chemical Reactions

Reactions of potential importance involving the geochemistry of the near-field environment of a HLW repository are homogeneous complexing reactions within the aqueous phase; reactions with minerals and solid compounds in the surrounding host rock, engineered barrier, including waste package and waste form, and other engineering materials; reactions with $O_{2(g)}$, $CO_{2(g)}$, H_2O, and other components of air; and formation of $H_{2(g)}$ resulting from anaerobic corrosion of the steel waste package. The reactions are all formulated in terms of a complete set of primary species A_j, with aqueous secondary species A_i, minerals or solid compounds A_m,and gases A_i^g. The primary species thus represent a set of independent chemical components. The reactions can thus be expressed in the following general forms for aqueous species, minerals, and gases:

$$\sum_{j=1}^{N_{\text{pri}}} \nu_{ji} A_j \rightleftharpoons A_i, \quad \left(i = 1, \ ..., \ N_{\text{cmplx}}\right) , \tag{2-69}$$

$$\sum_{j=1}^{N_{\text{pri}}} \nu_{jm} A_j \rightleftharpoons A_m, \quad \left(m = 1, \ ..., \ N_{\text{min}}\right) , \tag{2-70}$$

and

$$\sum_{j=1}^{N_{pri}} \nu_{ji}^{g} A_j \rightleftharpoons A_i^{g}, \quad (i = 1, \ldots, N_g) \ . \tag{2-71}$$

Here, N_{pri} denotes the number of primary species, N_{cmplx} the number of aqueous secondary species, N_{min} the number of minerals, and N_g the number of gases. The stoichiometric reaction matrices ν_{ji}, ν_{jm} and ν_{ji}^{g} give the number of moles of the jth primary species in one mole of the ith aqueous complex, mth mineral, and ith gas, respectively. The corresponding rates of reaction, taken as positive for reaction to the right and negative to the left, are denoted by I_i, I_m, and I_i^g, respectively. In the system Na–Cl–H_2O, examples of primary and secondary species are the sets of species (Na^+, H^+, Cl^-, H_2O) and (NaCl°, NaOH°, OH^-), respectively.

In addition, ion-exchange reactions may take place between the aqueous solution and solid phases. The possible exchange reactions include exchange between primary and secondary species. The different possibilities are shown in the Table 2-1. The exchange reactions may take place between primary species

$$z_{j'} A_j + z_j X_{z_j}^{\alpha} A_{j'} \rightleftharpoons z_j A_{j'} + z_{j'} X_{z_j}^{\alpha} A_j \quad (j \rightleftharpoons j') \ , \tag{2-72}$$

primary and secondary species

$$z_i A_j + z_j X_{z_i}^{\alpha} A_i \rightleftharpoons z_j A_i + z_i X_{z_j}^{\alpha} A_j \quad (j \rightleftharpoons i) \ , \tag{2-73}$$

and secondary species

$$z_{i'} A_i + z_i X_{z_{i'}}^{\alpha} A_{i'} \rightleftharpoons z_i A_{i'} + z_{i'} X_{z_i}^{\alpha} A_i \quad (i \rightleftharpoons i') \ . \tag{2-74}$$

where solid exchange sites are denoted by the hypothetical species X^{α}. The valence of the lth species is denoted by z_l. For exchange of a species with valence z, X_x^{α} exchange sites are occupied. The respective exchange rates are denoted by I_{ji}, $I_{jj'}$, and $I_{ii'}$. They satisfy the antisymmetry condition

$$I_{ji} = -I_{ij} \ , \tag{2-75}$$

with similar relations for $I_{jj'}$ and $I_{ii'}$. Describing ion-exchange reactions in the presence of mineral precipitation and dissolution reactions can become complicated because the surfaces on which exchange reactions are taking place may be dissolving or forming new layers, for example.

Table 2-1. Possible exchange reactions involving primary and secondary species.

Indices	Species Types
j,j'	Primary-primary
j,i	Primary-secondary
i,i'	Secondary-secondary

2.2.2 Sources and Sinks

Sources and sinks are provided by the chemical reaction rates I_i, I_m, and I_i^g, and ion-exchange rates $I_{jj'}$, I_{ji}, and $I_{ii'}$. The rate of reaction may be surface controlled with the reaction in disequilibrium, or transport controlled with the reaction representing conditions of local chemical equilibrium. For transport controlled conditions, additional algebraic relations must be imposed on the system to represent equilibrium replacing kinetic formulations.

2.2.2.1 Mass Conservation Equations for Reactive Transport

Mass conservation equations for each species - aqueous, mineral, and gas - can be written taking into account the chemical reactions described above. The transport equations take the following form for primary species

$$\frac{\partial}{\partial t}\left(\phi S_l C_j^l\right) + \nabla \cdot \boldsymbol{J}_j^l = -\sum_i \nu_{ji} I_i - \sum_m \nu_{jm} I_m - \sum_i \nu_{ji}^g I_i^g - \sum_\alpha \sum_{j' \neq j} z_{j'} I_{jj'}^\alpha - \sum_\alpha \sum_i z_i I_{ji}^\alpha \,, \tag{2-76}$$

for aqueous secondary species

$$\frac{\partial}{\partial t}\left(\phi S_l C_i^l\right) + \nabla \cdot \boldsymbol{J}_i^l = I_i + \sum_\alpha \sum_j z_j I_{ji}^\alpha + \sum_\alpha \sum_{i' \neq i} z_{i'} I_{ii'}^\alpha \,, \tag{2-77}$$

for gases

$$\frac{\partial}{\partial t}\left(\phi S_g C_i^g\right) + \nabla \cdot \boldsymbol{J}_i^g = I_i^g \,, \tag{2-78}$$

and for minerals

$$\frac{\partial}{\partial t}\left(\phi_m \bar{V}_m^{-1}\right) = I_m \,. \tag{2-79}$$

For ion-exchanged primary species, the transport equations are given by

$$\frac{\partial}{\partial t}\left(\bar{C}_j^{\alpha}\right) = \sum_{j' \neq j} z_{j'} I_{jj'}^{\alpha} + \sum_i z_i I_{ji}^{\alpha} \ , \tag{2-80}$$

and for ion-exchanged secondary species by

$$\frac{\partial}{\partial t}\left(\bar{C}_i^{\alpha}\right) = \sum_j z_j I_{ji}^{\alpha} + \sum_{i' \neq i} z_{i'} I_{ii'}^{\alpha} \ . \tag{2-81}$$

In these equations, $C_{j,i}^{l}$ represents the concentrations of primary and secondary aqueous species, C_i^{g} the concentration of gaseous species, $\bar{C}_{j,i}^{\alpha}$ represents the sorbed concentration of the subscripted species on sites labeled α, and J_i^{π} represents the flux of the π th species in the ith phase. The form of the flux term is discussed next.

2.2.2.2 Flux Term

The flux consists of contributions from diffusion and advection represented by Darcy's law. The Darcy flux (velocity) is given by

$$q_{\pi} = -\frac{k k_{r\pi}}{\mu_{\pi}}\left(\nabla p_{\pi} + \rho_{\pi} g \hat{z}\right) \ , \tag{2-82}$$

where k denotes the saturated permeability, $k_{r\pi}$ denotes the relative permeability, p_{π} denotes the pressure, μ_{π} represents the viscosity and ρ_{π} the density of phase π, g denotes the acceleration of gravity, and $\hat{z}$ represents a unit vector in the vertical direction. The mass flux resulting from the Darcy flow field can be expressed in either mass or mole units according to

$$J_i^{\pi\rho} = \rho_{\pi} w_i^{\pi} q_{\pi} \ , \tag{2-83}$$

or

$$J_i^{\pi c} = c_{\pi} x_i^{\pi} q_{\pi} \ , \tag{2-84}$$

respectively.

The diffusive flux may take several different forms depending on the phase and the pore dimensions of the porous medium in question. For the aqueous phase with species-independent diffusion coefficients and a sufficiently dilute solution, Fick's law may be used in the form

$$J_i^{D} = -\phi \tau D \nabla C_i \ , \tag{2-85}$$

where τ denotes the tortuosity and D represents the diffusion coefficient in an aqueous solution. This form becomes inadequate for more concentrated solutions and for the case when species-dependent diffusion coefficients are important.

2.2.3 Initial and Boundary Conditions

The mass transport equations are subject to initial and boundary conditions. For example, for a 1D porous column of length L, the initial and boundary conditions have the form

$$C_j(0,t) = C_j^0 \ , \tag{2-86}$$

$$C_j(x,0) = C_j^\infty \ , \tag{2-87}$$

and

$$\frac{\partial C_j}{\partial x}(L,t) = 0 \ , \tag{2-88}$$

for aqueous species. In addition, the initial solid composition must be specified.

$$\phi_m(x,0) = \phi_m^\infty \ , \tag{2-89}$$

and

$$\bar{C}_j^\alpha(x,0) = \bar{C}_j^{\alpha 0} \ , \tag{2-90}$$

for primary species and a similar relation for secondary species

$$\bar{C}_i^\alpha(x,0) = \bar{C}_i^{\alpha 0} \ . \tag{2-91}$$

2.2.4 Constitutive Relations

Various constitutive relations must be added to the transport equations to define the reaction rates for minerals, secondary species, and gases. For minerals, it is usually necessary to assume kinetic rate expressions, especially at lower temperatures. However, for aqueous complexes and gases, it is customary to assume conditions of local equilibrium. In this latter case, algebraic relations given by the corresponding mass action equations supplement the mass conservation equations. The mass action equations relate the concentrations of secondary species and gases to the concentrations of primary species. However, it should be noted that for redox reactions, in particular, the local equilibrium approximation may not be valid.

2.2.4.1 Aqueous, Mineral, and Gas Equilibria

The mass action equations corresponding to the chemical reactions appearing in Eqs. (2-69), (2-70), and (2-71) have the following forms for the aqueous secondary species:

$$C_i^l = \left(\gamma_i^l\right)^{-1} K_i \prod_{j=1}^{N_{\text{pri}}} \left(\gamma_j^l C_j^l\right)^{\nu_{ji}} , \tag{2-92}$$

stoichiometric minerals:

$$K_m \prod_{j=1}^{N_{\text{pri}}} \left(\gamma_j^l C_j^l\right)^{\nu_{jm}} = 1 , \tag{2-93}$$

and gases:

$$p_i^g = \left(\gamma_i^g\right)^{-1} K_i^g \prod_{j=1}^{N_{pri}} \left(\gamma_j^l C_j^l\right)^{\nu_{ji}^g} , \tag{2-94}$$

where p_i^g represents the partial pressure of the ith gaseous species, γ_k^l, γ_k^g denotes the activity and fugacity coefficients, respectively, of the kth species, and K_i, K_m, and K_i^g denote the respective equilibrium constants for secondary aqueous species, minerals, and gases.

A special case of the latter reactions is the evaporation and condensation of water. The assumption of local equilibrium implies the algebraic equilibrium constraint at the water-steam saturation curve given by

$$\mu_g(T,p) = \mu_l(T,p) , \tag{2-95}$$

where μ_g and μ_l denote the chemical potential of the gas and liquid, respectively. This equation simply specifies the pressure to lie along the saturation curve of pure water:

$$p = p_{\text{sat}}(T) , \tag{2-96}$$

where p_{sat} denotes the saturation pressure.

2.2.5 Reduced Mass Conservation Equations

The mass conservation equations may be simplified by eliminating those reaction rates that are governed by conditions of local chemical equilibrium. Because the concentrations of species that are assumed to be in local equilibrium can be computed directly from the concentrations of the primary species, it is not necessary to know the rates at which these species are formed. For each such species, there is one chemical reaction and associated rate representing its formation or depletion.

For conditions of local equilibrium, the reaction rates of secondary species, I_i, and gases, I_i^g may be eliminated from the transport equations for primary species by substituting Eqs. (2-77) and (2-78) into Eq. (2-76), resulting in the equation:

$$\frac{\partial}{\partial t}\left\{\phi\left[S_l\left(\Psi_j^l + \Phi_j\right) + S_g\Psi_j^g\right]\right\} + \nabla\cdot\left(\Omega_j^l + \Omega_j^g\right) = -\sum_{m=1}^{N_{\min}} \nu_{jm} I_m \,, \tag{2-97}$$

where the generalized concentration Ψ_j^π and flux Ω_j^π are defined by

$$\Psi_j^l = C_j^l + \sum_i \nu_{ji} C_i^l \,, \tag{2-98}$$

$$\Psi_j^g = \sum_i \nu_{ji}^g C_i^g \,, \tag{2-99}$$

and

$$\Omega_j^l = J_j^l + \sum_i \nu_{ji} J_i^l \,, \tag{2-100}$$

$$\Omega_j^g = \sum_i \nu_{ji}^g J_i^g \,, \tag{2-101}$$

and the ion-exchange concentration Φ_j by

$$\Phi_j = \sum_\alpha \left(\bar{C}_j^\alpha + \sum_i \nu_{ji}\bar{C}_i^\alpha\right) . \tag{2-102}$$

These equations are expressed entirely in terms of the concentrations of primary species alone. Combined with the mineral mass transfer equations, Eq. (3-79) and the appropriate algebraic equations representing the mass action equations of the eliminated reaction rates, these equations completely determine the time evolution of the system. The number of partial differential equations necessary to solve has been reduced to $N_{\text{pri}}+N_{\min}$. It should be noted that unlike the concentration C_j, the generalized concentration Ψ_j may take on positive or negative values.

If certain mineral reactions can be assumed to be in local equilibrium, their reaction rates can be eliminated from the primary species transport equations and the mineral mass transfer equations replaced by the corresponding mass action equations. Dividing the set of minerals into reversibly and irreversibly reacting minerals with

$$N_{\min} = N_{\min}^{\text{rev}} + N_{\min}^{\text{irr}} , \tag{2-103}$$

and eliminating the reversible rates from the primary species transport equations leads to an alternative form of the primary species conservation equations given by

$$\frac{\partial}{\partial t}\left\{\phi\left[S_l\left(\Psi_j^l + \Phi_j\right) + S_g \Psi_j^g\right] + \sum_{m=1}^{N_{\min}^{\text{rev}}} \nu_{jm}^{\text{rev}} \bar{V}_m^{-1} \phi_m^{\text{rev}}\right\} + \nabla\cdot\left[\mathbf{\Omega}_j^l + \mathbf{\Omega}_j^g\right] = -\sum_{m=1}^{N_{\min}^{\text{irr}}} \nu_{jm}^{\text{irr}} I_m^{\text{irr}} , \tag{2-104}$$

where the only remaining reaction rates are those corresponding to irreversibly reacting minerals, all other rates having been eliminated. These equations combined with the mineral mass transfer equations for irreversibly reacting minerals and the appropriate constitutive relations for reversibly reacting minerals, completely determine the time evolution of the system. If desired, the eliminated rates of reaction of the reversible species (aqueous species, gases, and minerals) can be determined by differentiation after the transport equations have been solved.

The reduction of the primary species transport equations may be taken one step further by eliminating all mineral reaction rates on the right hand side of Eq. (2-97) by substituting the mineral mass transfer equations given by Eq. (2-79) for the rates. This substitution results in the partial differential equation

$$\frac{\partial}{\partial t}\left\{\phi\left[S_l\left(\Psi_j^l + \Phi_j\right) + S_g \Psi_j^g\right] + \sum_{m=1}^{N_{\min}} \nu_{jm} \bar{V}_m^{-1} \phi_m\right\} + \nabla\cdot\left[\mathbf{\Omega}_j^l + \mathbf{\Omega}_j^g\right] = 0 , \tag{2-105}$$

in which all reaction rates have been eliminated. This form of the primary species transport equations may offer some numerical advantages compared to the other forms when using operator splitting techniques in solving these equations in two or three spatial dimensions.

2.2.6 Energy Conservation Single Fluid Phase

2.2.6.1 Energy Conservation Equation

The energy conservation equation has the form:

$$\frac{\partial}{\partial t}\left\{(1-\phi)\rho_{\text{rock}} C_{\text{rock}} T + \phi \sum_{\pi} S_\pi \rho_\pi^0 u_\pi\right\} + \nabla\cdot\boldsymbol{J} = 0 , \tag{2-106}$$

where the heat flux term is given by

$$J = -\kappa \nabla T + \sum_{\pi,i} h_i^{\pi} J_i^{\pi} , \tag{2-107}$$

where κ denotes the effective thermal conductivity of the bulk medium saturated with liquid and gas at local thermal equilibrium (Nield and Bajany, 1992). In general, the thermal conductivity is a function of saturation. Note that the enthalpy occurs in the flux term rather than internal energy to account for pV work in moving the fluid. This equation is based on the assumption that the rock and fluid are in thermal equilibrium. Internal energy and enthalpy are related by the thermodynamic equation:

$$h_{\pi} = u_{\pi} + \frac{p_{\pi}}{\rho_{\pi}^{0}} . \tag{2-108}$$

2.2.6.2 Sources and Sinks

In general, chemical reactions can contribute to the source of heat in addition to radioactive waste. However, with the exception of evaporation and condensation of H_2O, contributions from chemical reactions are expected to be minor by comparison and therefore are not considered further.

2.2.7 Two-Phase Water—Steam Transport: Evaporation and Condensation

The chemical reaction of primary importance in the near-field environment of a HLW repository is evaporation and condensation of water vapor described by the reaction

$$H_2O_{(l)} \rightleftharpoons H_2O_{(g)} . \tag{2-109}$$

Denoting the rate of this reaction by I_{H_2O}, then $I_{H_2O} > 0$ refers to the rate of evaporation and $I_{H_2O} < 0$, the rate of liquid condensation.

A mathematical description of evaporation and condensation of water for conditions of local equilibrium follows directly from the mass and energy conservation equations with no additional assumptions. The mass and energy conservation equations read for the vapor phase:

$$\frac{\partial}{\partial t} \phi S_g \rho_w^g + \nabla \cdot J_w^g = I_{H_2O} , \tag{2-110}$$

the liquid phase:

$$\frac{\partial}{\partial t} \phi S_l \rho_w^l + \nabla \cdot J_w^l = -I_{H_2O} , \tag{2-111}$$

and thermal energy:

$$\frac{\partial}{\partial t}\left[(1-\phi)C_P^{\text{rock}}T + \phi\left(\rho_w^l u_l + \rho_w^g u_g\right)\right] + \nabla\cdot\left(h_l J_w^l + h_g J_w^g\right) - \nabla\cdot\mathrm{K}\nabla T = 0\ . \tag{2-112}$$

In addition to these differential equations, the assumption of local equilibrium implies the algebraic equilibrium constraint at the water-steam saturation curve given by Eq. (2-96). Together, these equations provide four equations in the four unknowns: p, T, S_g, and $I_{\mathrm{H_2O}}$.

These equations may be simplified by adding Eqs. (2-110) and (2-111) to yield the single equation

$$\frac{\partial}{\partial t}\left[\phi\left(S_g\rho_w^g + S_l\rho_w^l\right)\right] + \nabla\cdot\left(J_w^g + J_w^l\right) = 0\ . \tag{2-113}$$

This equation coupled with the energy conservation equation gives two equations in the two unknowns T and S_g, with the pressure fixed at the saturation curve: $p = p_{sat}(T)$. This is the procedure used by the computer code V-TOUGH (Nitao, 1990), in which local equilibrium of liquid and vapor is stipulated. The relation between the independent field variables and the phase state of water is given in Table 2-2.

Once the transport equations have been solved the rate of condensation/evaporation can be obtained by differentiation:

$$I_{\mathrm{H_2O}} = -\left[\frac{\partial}{\partial t}\phi S_l\rho_w^l + \nabla\cdot J_w^l\right] = \frac{\partial}{\partial t}\phi S_g\rho_w^g + \nabla\cdot J_w^g\ . \tag{2-114}$$

The condensation/evaporation rate has the units of kg $\mathrm{m^{-3}\ s^{-1}}$.

A pseudo-kinetic description of condensation and evaporization is also possible in principal. In this case, the rate $I_{\mathrm{H_2O}}$ is expressed, for example, as

$$I_{\mathrm{H_2O}} = k\left[p - p_{\mathrm{sat}}(T)\right]\ , \tag{2-115}$$

where k denotes an effective rate constant. The local equilibrium description is retrieved in the limit $k\to\infty$. This approach is apparently used in the computer code PORFLOW (Runchal and Sagar, 1992). However, in this case, the unknown variables are p, T, and S_g, one more than in the local equilibrium case since pressure is no longer fixed at the saturation curve, but instead must be solved for.

2.3 SIMPLIFIED SYSTEM: $\mathrm{NaCl-H_2O}$

It is instructive to write out the mass conservation equations explicitly for the simplified system $\mathrm{NaCl-H_2O}$, including precipitation and dissolution of halite. Three chemical reactions are considered:

Table 2-2. Water-steam phase transition relations

Phase(s)	Saturation State	Pressure-Temperature Relation	Independent Field Variables
Liquid	$S_l=1,\ S_g=0$	$p>p_{sat}(T)$	$T,\ p$
Gas	$S_l=0,\ S_g=1$	$p<p_{sat}(T)$	$T,\ p$
Liquid+gas	$S_l,\ S_g>0,\ S_l+S_g=1$	$p=p_{sat}(T)$	$T,\ S_g$

water evaporation and condensation

$$H_2O_{(l)} \rightleftharpoons H_2O_{(g)} , \tag{2-116}$$

aqueous complexing

$$Na^+ + Cl^- \rightleftharpoons NaCl^0 , \tag{2-117}$$

and precipitation and dissolution of halite

$$Na^+ + Cl^- \rightleftharpoons NaCl_{(s)} . \tag{2-118}$$

The mass conservation equations for H_2O, Na^+, and Cl^- are given by

$$\frac{\partial}{\partial t}\left[\phi\left(S_g \rho_w^g + S_l \rho_w^l\right)\right] + \nabla \cdot \left(J_w^g + J_w^l\right) = 0 , \tag{2-119}$$

$$\frac{\partial}{\partial t}\left[\phi S_l\left(C_{Na^+} + C_{NaCl^0}\right)\right] + \nabla \cdot \left(N_{Na^+} + N_{NaCl^0}\right) = -I_{NaCl_s} , \tag{2-120}$$

and

$$\frac{\partial}{\partial t}\left[\phi S_l\left(C_{Cl^-} + C_{NaCl^0}\right)\right] + \nabla \cdot \left(N_{Cl^-} + N_{NaCl^0}\right) = -I_{NaCl_{(s)}} , \tag{2-121}$$

where $J_w^{l,g}$ refers to the flux in mass units, and N_i denotes the flux represented by mole units. The equation for the solvent water is coupled to the solute transport equations through the molality of the sodium and chloride species. For halite, one has the mass transfer equation

$$\frac{\partial}{\partial t}\phi_{NaCl_{(s)}} = \bar{V}_{NaCl_{(s)}} I_{NaCl_{(s)}} , \tag{2-122}$$

giving the amount of halite precipitated or dissolved as a function of time at each point in space.

2.3.1 V-TOUGH

The mass and energy conservation equations solved by V-TOUGH for species water (*w*), air (*a*), and thermal energy have the form:

water:

$$\frac{\partial}{\partial t}\left[\phi\left(\rho_l S_l w_w^l + \rho_g S_g w_w^g\right)\right] + \nabla \cdot \left(w_w^l F_l + w_w^g F_g + F_w^D + F_w^K\right) = Q_w , \tag{2-123}$$

air:

$$\frac{\partial}{\partial t}\left[\phi\left(\rho_l S_l w_a^l + \rho_g S_g w_a^g\right)\right] + \nabla \cdot \left(w_a^l F_l + w_a^g F_g + F_a^D + F_a^K\right) = Q_a , \tag{2-124}$$

and thermal energy:

$$\frac{\partial}{\partial t}\left[(1-\phi)C_{\text{rock}}T + \phi\left(\rho_l S_l u_l + \rho_g S_g u_g\right)\right] + \nabla\cdot\left(-\mathrm{K}_{\text{rock}}\nabla T + h_l F_l + h_g F_g + h_w^g F_w^D + h_a^g F_a^D\right) = Q_{\text{rock}} + h_w Q_w + h_a Q_a . \tag{2-125}$$

In these equations, the various Q-terms represent sources and sinks for the respective species and heat, and F_i denotes the flux of the respective species.

2.3.2 Comparison of V-TOUGH and PORFLOW

There is a discrepancy in the form of the energy balance equation used by different computer codes. In the code PORFLOW (Runchal and Sagar, 1993), the enthalpy appears in the accumulation term rather than the internal energy, whereas V-TOUGH uses internal energy. This could result in significant differences between the two codes. The time derivative of the difference in internal energy and enthalpy is noted here to be given by:

$$\frac{\partial}{\partial t}\left[\phi \sum_{\pi} S_{\pi} \rho_{\pi}\left(h_{\pi} - u_{\pi}\right)\right] = \sum_{\pi} \frac{\partial}{\partial t}\left(\phi S_{\pi} p_{\pi}\right) , \tag{2-126}$$

recalling that

$$h_{\pi} = u_{\pi} + p_{\pi} V_{\pi} = u_{\pi} + \frac{p_{\pi}}{\rho_{\pi}} . \tag{2-127}$$

For the case that the pressure is the same for all fluid phases, this expression reduces to

$$\frac{\partial}{\partial t}\left[\phi \sum_{\pi} S_{\pi} \rho_{\pi}\left(h_{\pi} - u_{\pi}\right)\right] = \frac{\partial}{\partial t}\left(\phi p\right) . \tag{2-128}$$

The use of enthalpy rather than internal energy in the time-derivative term is seen to affect only the transient behavior of the system. The internal energy formulation would, however, appear to be the correct form of the energy balance equation. This would necessitate a minor change to PORFLO to include the internal energy in the accumulation term.

3 MULTICOMPONENT DIFFUSION OF GAS IN A POROUS MEDIUM

This chapter reviews the dusty gas model (DGM) for gaseous diffusion and presents a derivation of some of the relevant equations. In particular, an explicit expression is derived for the diffusive flux for a binary system.

For multicomponent gaseous systems at either low pressure or in small pores, Fick's law of diffusion is generally inapplicable, and it is necessary to consider a more comprehensive theory that involves Knudsen diffusion. In such circumstances, the mean free path of a gas molecule is long compared to the size of a pore. Such a theory is provided by the so-called DGM developed by Mason and coworkers beginning in the mid-1960s (Mason et al., 1967; Gunn and King, 1969; Cunningham and Williams, 1980; Mason and Malinauskas, 1983; Thorstenson and Pollock, 1989a, b). The DGM receives its name from the approach used to describe the solid phase portion of a porous medium as consisting of giant (compared to the size of a molecule) motionless particles. This theory is based on a first-order perturbation analysis of the Boltzmann equation. Diffusion can result in both segregation of the diffusing gas molecules, as in the usual continuum theory of diffusion based on Fick's law, and bulk flow of gas—so-called *diffusion caused advection*. The constitutive relations for the flux involve competition between Knudsen diffusion, continuum or molecular diffusion, and bulk Darcy flow of gas in a porous medium.

An estimate of pore diameters for which Knudsen diffusion is expected to be important is provided by the Knudsen number defined as the ratio of the molecular mean free path to the pore diameter. The mean free path λ of a gas molecule is defined as

$$\lambda = \frac{1}{\sqrt{2}\sigma n} , \tag{3-1}$$

where σ denotes the collision cross section

$$\sigma = \pi d^2 , \tag{3-2}$$

with d the diameter of the gas molecules, and n refers to the number density of the gas. For an ideal gas

$$n = \frac{N}{V} = \frac{N_A P}{RT} , \tag{3-3}$$

where N is the total number of molecules and N_A represents Avogadro's number. The Knudsen number can be expressed as

$$Kn = \frac{\lambda}{l} . \tag{3-4}$$

for pore diameter l. The mean free path in air is approximately 6.6×10^{-6} cm (Vincenti and Kruger, 1965) at 25 °C and 1 atmosphere.

Molecular diffusion dominates for $Kn<1$, and Knudsen diffusion for $Kn>1$. Knudsen diffusion may become important for pore sizes less than a micrometer at atmospheric pressure. Ali et al. (1993) have concluded, based on measurements of the effective diffusion coefficient of CO_2 gas in Yucca Mountain tuff, that diffusive transport of CO_2 through Topopah Spring tuffs may occur in the transition regime between Knudsen and molecular diffusion.

Fick's law of diffusion and bulk flow resulting from diffusion (Bird et al., 1960), follow as limiting cases of the DGM for high ambient pressure and large pore sizes. Numerical computer codes such as V-TOUGH (Nitao, 1990) and PORFLOW (Runchal and Sagar, 1993) are based on a Fickian formulation of the diffusive flux combined with Darcy's law. Use of Fick's law for diffusion of gas in porous media with sufficiently low permeability, however, may underestimate evaporation rates by several orders of magnitude.

3.1 REFERENCE FRAMES

A fundamental description of diffusion is based on transport relative to a frame of reference moving with the bulk fluid velocity. For the case of diffusion of solute species in a solvent, such as water in which the solvent provides a unique bulk fluid velocity, Fick's law is appropriate. However, in the case of transport of gases, a unique definition of the bulk flow velocity may not exist, and a consistent definition of diffusion must take this into account. Following Bird et al. (1960), diffusive transport is defined relative to the average bulk fluid velocity based on mass, mole-number or volume averages.

Consider a multiphase system with local velocity of the *i*th species in fluid phase π denoted by v_i^π. Then the average local velocity of the phase π can be expressed in various ways, depending on the type of averaging employed (see Table 3-1 for notation). Three distinct average phase velocities may be defined corresponding to mass, mole-number, and volume averages. The local mass average velocity v_π^ρ is defined by:

$$v_\pi^\rho = \frac{\sum_i \rho_i^\pi v_i^\pi}{\rho_\pi}, \tag{3-5}$$

the mole-number average velocity by:

$$v_\pi^c = \frac{\sum_i c_i^\pi v_i^\pi}{c_\pi}, \tag{3-6}$$

and the volume average velocity by the expression:

$$v_\pi^\phi = \frac{\sum_i V_i^\pi v_i^\pi}{V_\pi}. \tag{3-7}$$

Table 3-1. Notation for the bulk fluid velocity in different representations of concentration variables

Representation	Concentration	Fractional Unit	Bulk Fluid Velocity
Mass	ρ_i	w_i	v^{ρ}
Mole-number	c_i	x_i	v^{c}
Volume	V_i	ϕ_i	v^{ϕ}

In these expressions, ρ_{π}^{0} is the mass density, c_{π} is the molar density of phase π, ρ_i^{π} is the mass density, and c_i^{π} the molar concentration of the ith species in phase π. The quantity V_{π} denotes the volume of a REV of phase π, and V_i^{π} denotes the volume of the ith species in phase π related to the partial molar volume $\overline{V}_i^{\pi}$ by the expression

$$V_i^{\pi} = n_i^{\pi}\overline{V}_i^{\pi} \ . \tag{3-8}$$

Introducing the species flux defined relative to a fixed coordinate system F_i^{ρ}, F_i^{c}, and F_i^{ϕ} defined by

$$\begin{aligned} F_i^{\rho} &= \rho_i v_i \ , \\ F_i^{c} &= c_i v_i \ , \\ F_i^{\phi} &= V_i v_i \ , \end{aligned} \tag{3-9}$$

where the superscript designating the phase π is dropped for convenience, the bulk fluid velocities can be expressed as

$$\begin{aligned} v^{\rho} &= \frac{1}{\rho}\sum F_i^{\rho} \ , \\ v^{c} &= \frac{1}{c}\sum F_i^{c} \ , \\ v^{\phi} &= \frac{1}{V}\sum F_i^{\phi} \ . \end{aligned} \tag{3-10}$$

The mole-number and mass average bulk velocities are related by the expression

$$v_{\pi}^{c} = f_{\pi} v_{\pi}^{\rho} \ , \tag{3-11}$$

where the factor f_π is given by

$$
\begin{aligned}
f_\pi &= \frac{\sum_i x_i^\pi v_i^\pi}{\sum_l w_l^\pi v_l^\pi} , \\
&= \frac{\left(\sum_i x_i^\pi v_i^\pi\right)\left(\sum_j M_j x_j^\pi\right)}{\sum_l M_l x_l^\pi v_l^\pi} , \\
&= \frac{\sum_l M_l^{-1} w_l^\pi v_l^\pi}{\left(\sum_i w_i^\pi v_i^\pi\right)\left(\sum_j M_j^{-1} w_j^\pi\right)} ,
\end{aligned}
\tag{3-12}
$$

for different representations of combined mass-mole fraction, mole and mass fraction, where x_i^π denotes the mole fraction and w_i^π denotes the mass fraction. The quantity f_π clearly depends on the composition of the fluid phase π.

The volume average bulk velocity can be expressed in the form

$$
v^\phi = \sum_i \chi_i^\pi v_i^\pi , \tag{3-13}
$$

with

$$
\begin{aligned}
\chi_i^\pi &= \bar{V}_i^\pi M_i^{-1} \rho_i^\pi , \\
&= \rho_\pi \bar{V}_i^\pi M_i^{-1} w_i^\pi , \\
&= c_\pi \bar{V}_i^\pi x_i^\pi .
\end{aligned}
\tag{3-14}
$$

3.2 DIFFUSIVE FLUX

The diffusive flux is defined relative to a frame of reference that is at rest with respect to the local bulk fluid velocity. This definition leads to the following expressions for the diffusive flux corresponding to the different representations of the bulk velocity:

$$J_i^{\rho} = \rho_i \left(v_i - v^{\rho}\right) = -D\rho \nabla w_i ,$$
$$J_i^{c} = c_i \left(v_i - v^{c}\right) = -Dc \nabla cx_i , \qquad (3\text{-}15)$$
$$J_i^{\phi} = \phi_i \left(v_i - v^{V}\right) = -DV \nabla \phi_i ,$$

for mass, mole-number, and volume average bulk flow velocities, where D denotes the diffusion coefficient which is the same for all representations. In this equation, it is assumed that the diffusion coefficients are the same for all species for convenience.

By definition

$$\sum J_i^{\rho,c,v} = 0 \qquad (3\text{-}16)$$

Many other representations are possible involving mixed mass, mole, and volume representations (Bird et al., 1960). All these forms of the diffusive flux are equivalent, and any one may be used to describe the system completely. To prove this statement, consider the mass and mole-number formulations. It follows that

$$J_i^{\rho} = F_i^{\rho} - w_i \sum_l F_l^{\rho} , \qquad (3\text{-}17)$$

and similarly

$$J_i^{c} = F_i^{c} - x_i \sum_l F_l^{c} . \qquad (3\text{-}18)$$

Clearly

$$F_i^{\rho} = M_i F_i^{c} . \qquad (3\text{-}19)$$

In addition, multiplying Eq. (3-17) by M_i and subtracting Eq. (3-16) yields

$$M_i J_i^{c} = J_i^{\rho} + \rho_i \left(v^{\rho} - v^{c}\right) . \qquad (3\text{-}20)$$

Summing over i gives:

$$\sum_i M_i J_i^{c} = \rho \left(v^{\rho} - v^{c}\right) , \qquad (3\text{-}21)$$

and the difference in the bulk flow mass and mole-number-based velocities can be expressed as

$$v^{\rho} - v^{c} = \frac{1}{\rho} \sum_i M_i J_i^{c} . \qquad (3\text{-}22)$$

It follows from Eq. (3-19) that J_i^ρ can be expressed as

$$\begin{aligned} J_i^\rho &= M_i J_i^c - \rho_i\left(v^\rho - v^c\right) , \\ &= M_i J_i^c - w_i \sum_l M_l J_l^c . \end{aligned} \tag{3-23}$$

Substituting for J_i^c yields the expression

$$\begin{aligned} J_i^\rho &= -cD\left(M_i \nabla x_i - w_i \sum_l M_l \nabla x_l\right) , \\ &= -\rho D \nabla w_i , \end{aligned} \tag{3-24}$$

as follows by differentiating Eq. (2-16) and using Eq. (2-28), for the relation between c and ρ proving the desired result.

3.3 DUSTY GAS MODEL

In the DGM, the total flux F of a gas mixture in a porous medium is represented as the sum of two terms: the flux resulting from diffusion and the flux due to viscous forces (Gunn and King, 1969). For the ith species, the total flux is defined according to the equation

$$F_i = c_i v_i = F_i^D + F_i^V . \tag{3-25}$$

The viscous flux F_i^V satisfies the relation

$$F_i^V = x_i F^V , \tag{3-26}$$

with F^V represented by Darcy's law:

$$F^V = -c\frac{k}{\mu}\nabla P = -\frac{kP}{RT\mu}\nabla P , \tag{3-27}$$

where k represents the permeability of the gas mixture, μ the viscosity, and P denotes the total fluid pressure. The viscous flux is nonsegregative, that is, it acts on all species equally and does not lead to a separation in concentration of the gas constituents.

According to the DGM, the constitutive relation for the diffusive flux F_i^D, expressed in the molecular representation of concentration, is given by the equation

$$-\nabla c_i = \frac{1}{D_i^K} F_i^D - \sum_{j \neq i} \frac{1}{D_{ij}} \left(x_i F_j^D - x_j F_i^D \right) , \tag{3-28}$$

where D_i^K denotes the Knudsen diffusion coefficient, and D_{ij} denotes the continuum diffusion coefficient. The continuum diffusion coefficient is symmetric:

$$D_{ij} = D_{ji} . \tag{3-29}$$

The diffusive flux may be divided into segregative and nonsegregative contributions corresponding to diffusion and bulk flow of fluid, respectively,

$$F_i^D = J_i + F_i^N , \tag{3-30}$$

where J_i represents the segregative, and F_i^N the nonsegregative component. The pure diffusive segregative flux is defined relative to the bulk fluid velocity:

$$\begin{aligned} J_i &= c_i \left(v_i - v^c \right) , \\ &= F_i - x_i F . \end{aligned} \tag{3-31}$$

It follows that

$$\sum_i J_i = 0 . \tag{3-32}$$

The nonsegregative diffusive flux F^N is then given by

$$\begin{aligned} F_i^N = x_i F^N &= F_i^D - J_i , \\ &= F_i^D - \left(F_i - x_i F \right) , \\ &= F_i^D - \left(F_i^D - x_i F^D \right) = x_i F^D . \end{aligned} \tag{3-33}$$

The latter relation follows from the nonsegregative nature of the viscous flux. From this relation it follows that

$$\sum_i F_i^N = F^N = F^D . \tag{3-34}$$

The total flux F_i is the sum of the segregative pure diffusive flux J_i, the nonsegregative diffusive flux F_i^N, and the viscous Darcy flux F_i^V:

$$F_i = F_i^D + x_i F^V ,$$
$$= J_i + x_i F^N + x_i F^V . \tag{3-35}$$

For a multicomponent system, the pure diffusive flux can be calculated from the total fluxes using the expression

$$J_i = \sum_j \left(x_j F_i - x_i F_j \right) = F_i - x_i F$$
$$= \sum_j \left(x_j F_i^D - x_i F_j^D \right) , \tag{3-36}$$

where the latter expression follows because the viscous flux is nonsegregative and therefore cancels out.

With these relations for the flux, it follows that the bulk fluid velocity has the form

$$v^c = \frac{1}{c} \sum_i c_i v_i = \frac{1}{c} F ,$$
$$= \frac{1}{c} F^D + \frac{1}{c} F^V . \tag{3-37}$$

The Darcy velocity is given by the second term on the right hand side of the last expression:

$$v^c_{\text{Darcy}} = \frac{1}{c} F^V = -\frac{k}{\mu} \nabla P , \tag{3-38}$$

and a diffusion velocity can be identified with the first term

$$v^c_{\text{diff}} = \frac{1}{c} F^D = \frac{1}{c} F^N , \tag{3-39}$$

which is a consequence of the nonsegregative contribution to the diffusive flux. Thus it follows that

$$v^c = v^c_{\text{Darcy}} + v^c_{\text{diff}} . \tag{3-40}$$

According to this result, it is apparent that it is not correct to set the bulk velocity equal to the Darcy velocity alone, but an additional term results from diffusive processes. This formulation of diffusion is independent of the particular representation used, as it must be.

It should be noted that the diffusive flux is not simply given by Fick's law of diffusion. It is a much more complicated expression that reduces to Fick's law under the appropriate conditions discussed below, but also provides for bulk fluid motion resulting from diffusion alone. In terms of individual species fluid velocities, the diffusive flux J_i can be defined as above [see Eq. (3-30)], relative to a

coordinate system moving with the bulk velocity. But it is not possible, in general, to equate J_i with Fick's first law for diffusion as in Eq. (3-15).

The constitutive relations for the diffusive flux can be expressed in terms of the total and viscous, F_i and F_i^V, by writing

$$F_i^D = F_i - x_i F^V , \tag{3-41}$$

and noting that

$$x_i F_j^D - x_j F_i^D = x_i F_j - x_j F_i , \tag{3-42}$$

to yield:

$$-\nabla c_i = \frac{1}{D_i^K}\left(F_i + x_i \frac{kP}{RT\mu}\nabla P\right) - \sum_{j\neq i} \frac{1}{D_{ij}}\left(x_i F_j - x_j F_i\right) , \tag{3-43}$$

where the explicit form of the viscous flux given by Eq. (3-27) has been inserted. Summing this expression over i yields

$$-\nabla \sum_i c_i = \sum_i \frac{F_i^D}{D_i^K} . \tag{3-44}$$

This equation provides the basis for deriving Gramham's law of diffusion (Cunningham and Williams, 1980).

3.3.1 Explicit Form for the Diffusive Flux

Equation (3-28) forms the basis of the DGM applied to a system with walls, such as a porous medium. To use this equation in conjunction with mass or energy conservation equations, it is necessary to solve explicitly for the flux F_i^D. This can be done formally for an N-component system by writing Eq. (3-28) in the form:

$$\begin{aligned} -\nabla c_i &= \sum_j \left[\left(\frac{1}{D_j^K} + \sum_l \frac{x_l}{D_{il}} \right) \delta_{ij} - \frac{x_i}{D_{ij}} \right] F_j^D , \\ &= \sum_j \Gamma_{ij} F_j^D . \end{aligned} \tag{3-45}$$

where the matrix Γ_{ij} is defined by

$$\Gamma_{ij} = \left(\frac{1}{D_j^K} + \sum_l \frac{x_l}{D_{il}} \right) \delta_{ij} - \frac{x_i}{D_{ij}} . \tag{3-46}$$

Provided the matrix Γ_{ij} is nonsingular, this equation can be inverted to give formally

$$F_i^D = -\sum_j \left(\Gamma^{-1} \right)_{ij} \nabla c_j . \tag{3-47}$$

Although this equation appears to have the form of Fick's law, it is actually very different because of the dependence of Γ_{ij} on the concentration.

3.3.2 Binary Mixture

For a binary mixture, the equations for the DGM simplify greatly. In this case the DGM constitutive relations for the diffusive flux reduce to

$$-\nabla c_1 = \frac{1}{D_1^K} F_1^D - \frac{1}{D_{12}} \left(x_1 F_2^D - x_2 F_1^D \right) , \tag{3-48}$$

and

$$-\nabla c_2 = \frac{1}{D_2^K} F_2^D + \frac{1}{D_{12}} \left(x_1 F_2^D - x_2 F_1^D \right) . \tag{3-49}$$

These equations coupled with mass conservation equations and Darcy's law for the viscous contribution to the flux completely determine the evolution of the system. In matrix form, the DGM constitutive relations become

$$\begin{bmatrix} \left(\frac{1}{D_1^K} + \frac{x_2}{D_{12}} \right) & \frac{-x_1}{D_{12}} \\ -\frac{x_2}{D_{12}} & \left(\frac{1}{D_2^K} + \frac{x_2}{D_{12}} \right) \end{bmatrix} \begin{pmatrix} F_1^D \\ F_2^D \end{pmatrix} = - \begin{pmatrix} \nabla C_1 \\ \nabla C_2 \end{pmatrix} \tag{3-50}$$

The determinant of the coefficient matrix is given by

$$\det\Gamma = \frac{1}{D_1^K D_2^K}\left(1 + \frac{x_2 D_1^K + x_1 D_2^K}{D_{12}}\right). \tag{3-51}$$

For an ideal gas

$$c_i = x_i \frac{P}{RT}, \tag{3-52}$$

and it follows that for an isothermal system

$$\nabla c_i = \frac{P}{RT}\nabla x_i + \frac{x_i}{RT}\nabla P. \tag{3-53}$$

In this case, explicitly solving for F_1^D and F_2^D, yields

$$F_1^D = -\frac{D_1^K}{RT}\left[\frac{D_{12}P\nabla x_1 + x_1\left(D_{12} + D_2^K\right)\nabla P}{D_{12} + x_1 D_2^K + x_2 D_1^K}\right], \tag{3-54}$$

and

$$F_2^D = -\frac{D_2^K}{RT}\left[\frac{D_{12}P\nabla x_2 + x_2\left(D_{12} + D_1^K\right)\nabla P}{D_{12} + x_1 D_2^K + x_2 D_1^K}\right]. \tag{3-55}$$

The total diffusive flux is equal to

$$\begin{aligned} F^D &= F_1^D + F_2^D, \\ &= -\frac{1}{RT}\,\frac{D_{12}\left(D_1^K - D_2^K\right)P\nabla x_1 + \left[D_1^K D_2^K + D_{12}\left(x_1 D_2^K + x_2 D_1^K\right)\right]\nabla P}{D_{12} + x_1 D_2^K + x_2 D_1^K}. \end{aligned} \tag{3-56}$$

The pure segregative diffusive flux has the form:

$$\begin{aligned} J_1 &= x_2 F_1^D - x_1 F_2^D, \\ &= -\frac{D_{12}}{RT}\left[\left(x_2 D_1^K + x_1 D_2^K\right)P\nabla x_1 + x_1 x_2\left(D_1^K - D_2^K\right)\nabla P\right] \\ &\times \left(D_{12} + x_1 D_2^K + x_2 D_1^K\right)^{-1}. \end{aligned} \tag{3-57}$$

The nonsegregative diffusive flux is proportional to the total diffusive flux

$$F_1^N = x_1 F^D \ . \tag{3-58}$$

In the case where one of the gases is stagnant (e.g., $F_2 = 0$), a pressure gradient develops in the absence of any external forces. For the case of ideal gases, the pressure gradient satisfies the equation

$$\left[1 + \frac{D_{12}}{D_1^K} + \left(\frac{D_{12}}{D_1^K D_2^K} + \frac{x_1}{D_1^K} + \frac{x_2}{D_2^K}\right)\frac{kP}{\mu}\right]\nabla P = -\frac{D_{12}}{D_1^K}\frac{P}{x_2}\nabla x_2 \ , \tag{3-59}$$

with

$$F_2 = F_2^D + x_2 F^V = 0 \ . \tag{3-60}$$

This equation has been applied by Ünal (1987) to the system consisting of carbon dioxide diffusing through stagnant nitrogen at 25 °C.

3.3.3 Two Limiting Cases

Two limiting cases of the constitutive relations can be identified for large and small pressure based on the dimensionless ratio D_{12}/D_1^K. The Knudsen diffusion coefficient is independent of pressure, whereas the continuum diffusion coefficient is inversely proportional to the pressure:

$$D_{12} \sim \frac{1}{P} \ . \tag{3-61}$$

Therefore, the two limiting cases correspond to $D_{12} \ll D_i^K (P \to \infty)$ and $D_{12} \gg D_i^K (P \to 0)$. To analyze these limiting areas, it is useful to write the total flux for species 1 and 2 as

$$F_1 = -\frac{1}{1/D_1^K + 1/D_{12}}\nabla c_1 + x_1\left(\frac{1}{1 + D_{12}/D_1^K}F + \frac{1}{1 + D_1^K/D_{12}}F^V\right) , \tag{3-62}$$

and

$$F_2 = -\frac{1}{1/D_2^K + 1/D_{12}}\nabla c_2 + x_2\left(\frac{1}{1 + D_{12}/D_2^K}F + \frac{1}{1 + D_2^K/D_{12}}F^V\right) . \tag{3-63}$$

Case (i) $D_{12} > D_i^K$ $(P \to 0)$:

In this case, the flux becomes (free molecular limit):

$$F_1 = -D_1^K \nabla c_1 , \tag{3-64}$$

which is just Fick's law with the Knudsen diffusion coefficient.

Case (i) $D_{12} < D_i^K (P \to \infty)$:

In this case, the flux becomes (continuum limit):

$$F_1 = -D_{12} \nabla c_1 + x_1 F , \tag{3-65}$$

and

$$F_2 = -D_{12} \nabla c_2 + x_2 F . \tag{3-66}$$

This latter relation has been discussed by Bird et al. (1960) and includes a *diffusion-caused advection* term corresponding to the second term on the right hand side resulting in bulk fluid motion caused by diffusion. Bird et al. (1960) apply these equations to the case where one of the gases is stagnant (e.g., $F_2 = 0$). The equations then reduce to

$$F_1 = -\frac{D_{12}}{1 - x_1} \nabla c_1 , \tag{3-67}$$

and the bulk velocity in the molecular representation is given by

$$v^c = \frac{1}{c} F = \frac{1}{c} F_1 = -\frac{D_{12}}{1 - x_1} \nabla x_1 . \tag{3-68}$$

Fick's law can be retrieved in this case as follows from Eq. (3-56) which becomes for $D_{12} < D_i^K$

$$J_1 = -\frac{D_{12} P}{RT} \nabla x_1 - \frac{D_{12}}{RT} \frac{x_1 x_2 \left(D_1^K - D_2^K \right)}{x_1 D_2^K + x_2 D_1^K} \nabla P . \tag{3-69}$$

For equal Knudsen diffusivities, the pressure gradient term vanishes and Fick's law applies.

3.3.4 Equal Diffusion Coefficients

In this section the special case of equal continuum and Knudsen diffusion coefficients is considered. Thus, it is assumed that:

$$D_{ij} = D \ , \tag{3-70}$$

and

$$D_i^K = D_K \ . \tag{3-71}$$

The constitutive relations, Eq. (3-42), become

$$-D\nabla c_i = \left(1 + \frac{D}{D_K}\right) F_i + x_i \frac{D}{D_K} \frac{kP}{RT\mu} \nabla P - x_i F \ . \tag{3-72}$$

Summing over i gives the result

$$F = -\left(\frac{D_K}{RT} + \frac{kP}{RT\mu}\right) \nabla P \ , \tag{3-73}$$

noting that

$$\sum \nabla c_i = \nabla \sum c_i = \frac{1}{RT} \nabla P \ . \tag{3-74}$$

Substituting this result back into Eq. (3-72) and solving for F_i yields

$$F_i = -\frac{1}{1 + D/D_K} \left\{ x_i \left[\frac{D_K}{RT} + \left(1 + \frac{D}{D_K}\right) \frac{kP}{RT\mu} \right] \nabla P + D\nabla c_i \right\} \ . \tag{3-75}$$

In this case, the diffusive flux J_i is given by

$$J_i = -\frac{DD_K}{D + D_K} \frac{P}{RT} \nabla x_i \ , \tag{3-76}$$

similar to Fick's law, with an effective diffusion coefficient D_e given by the harmonic mean of the Knudsen and binary diffusion coefficients

$$D_e = \frac{DD_K}{D + D_K} \ . \tag{3-77}$$

For $D_K \gg D$, $D_e = D$, and Fick's law applies with the usual binary diffusion coefficient.

4 PARTIALLY SATURATED POROUS MEDIA

4.1 RICHARDS' EQUATION

For an incompressible fluid, conservation of mass in a partially saturated porous medium in a single spatial dimension is expressed by the equation

$$\frac{\partial}{\partial t}(\rho \phi S_l) + \frac{\partial}{\partial x}(\rho u) = 0 , \tag{4-1}$$

where ϕ denotes the porosity, S_l the liquid saturation index, ρ the density of water, and u the Darcy velocity defined by

$$u = -\frac{k k_r}{\mu}\left(\frac{\partial p}{\partial x} - \rho g \cos\theta\right) , \tag{4-2}$$

where k denotes the absolute permeability, k_r denotes the relative permeability, μ denotes the dynamic viscosity, p denotes the fluid pressure, and θ denotes the angle between the direction of flow and the vertical. The positive x-axis points downward. The pressure is defined in terms of the hydraulic head h by the relation

$$p = \rho g h , \tag{4-3}$$

where g denotes the acceleration of gravity. In terms of h and S_l the flow equation neglecting gravity becomes

$$\frac{\partial}{\partial t}(\phi S_l) - \frac{\partial}{\partial x}\left(K k_r \frac{\partial h}{\partial x}\right) = 0 , \tag{4-4}$$

referred to as the Richards' (1931) equation, where the hydraulic conductivity K is defined by

$$K = \frac{k \rho g}{\mu} . \tag{4-5}$$

Introducing the diffusivity $D(S_l)$, defined by

$$D(S_l) = K k_r(S_l) \frac{dh(S_l)}{dS_l} , \tag{4-6}$$

a positive quantity, the flow equation may be cast in the form

$$\frac{\partial}{\partial t}(\phi S_l) = \frac{\partial}{\partial x}\left[D(S_l)\frac{\partial S_l}{\partial x}\right] , \tag{4-7}$$

valid for a homogeneous porous medium.

The transport equation is solved subject to initial and boundary conditions. Several forms are possible. In terms of the liquid saturation they are given by

$$S(x,0) = S_\infty \ , \tag{4-8}$$

and

$$S(0,t) = S_0 \ . \tag{4-9}$$

The flux boundary condition at $x = 0$ is given by

$$J_0 = \rho u_0 = \frac{\rho Q_0}{A} \ , \tag{4-10}$$

where A denotes the cross-sectional area of the porous medium normal to the direction of flow. Solving for the pressure gradient yields the condition

$$\left(\frac{\partial p}{\partial x}\right)_0 = \rho g \cos\theta - \frac{J_0 \mu}{\rho k k_r} \ . \tag{4-11}$$

4.1.1 van Genuchten Constitutive Relations

Using the van Genuchten model for capillary pressure, saturation S_l and capillary head h^C are related by the equation

$$S(h) = \left[1 + (\alpha h^C)^\beta\right]^{-\lambda} \ , \tag{4-12}$$

with

$$\lambda = 1 - \frac{1}{\beta} \ , \tag{4-13}$$

and

$$S = \frac{S_l - S_r}{1 - S_r} \ , \tag{4-14}$$

where S is referred to as the effective saturation, and S_r denotes the residual saturation of the porous medium. The inverse relation is given by

$$h^C(S) = \frac{1}{\alpha}\left(S^{-1/\lambda} - 1\right)^{1/\beta} \ . \tag{4-15}$$

The relative permeability is given by

$$k_r(h^C) = \frac{\left\{1 - (\alpha h^C)^{\beta-1}\left[1 + (\alpha h^C)^{\beta}\right]^{-\lambda}\right\}^2}{\left[1 + (\alpha h^C)^{\beta}\right]^{\lambda/2}} . \quad (4\text{-}16)$$

In terms of the effective saturation S, this expression reduces to

$$k_r(S) = \sqrt{S}\left[1 - \left(1 - S^{1/\lambda}\right)^{\lambda}\right]^2 . \quad (4\text{-}17)$$

It follows from Eq. (4-15) that dh^C/dS is equal to

$$\frac{dh^C}{dS} = \frac{1}{\alpha\beta\lambda}\left(S^{-1/\lambda} - 1\right)^{-\lambda} S^{-(1+\lambda)/\lambda} , \quad (4\text{-}18)$$

and

$$\frac{dk_r}{dS} = \left[1 - \left(1 - S^{1/\lambda}\right)^{\lambda}\right]\left\{\frac{1}{2\sqrt{S}}\left[1 - \left(1 - S^{1/\lambda}\right)^{\lambda}\right] + 2\sqrt{S}\left(S^{-1/\lambda} - 1\right)^{\lambda-1}\right\} . \quad (4\text{-}19)$$

The Topopah Spring unit at YM is characterized roughly by the parameters for the rock matrix and fracture network given in Table 4-1.

Table 4-1. Permeabilities, porosities, and van Genuchten parameters for the rock matrix and fracture network characterizing the Topopah Spring unit at Yucca Mountain

	K (m^2)	ϕ	α (m^{-1})	β	$\lambda = 1 - 1/\beta$
Matrix	1.9×10^{-18}	0.11	0.00567	1.798	0.443826
Fracture	1.0×10^{-11}	0.0018	1.2851	4.23	0.763593

4.2 QUASI-STATIONARY STATE TRANSPORT EQUATION

This section investigates the use of the quasi-stationary state approximation for solving the Richards' equation in the case of a wetting front propagating through a partially saturated porous medium. The quasi-stationary state transport equation is given by

$$\frac{d}{dx}\left[\tilde{D}(S)\frac{dS}{dx}\right] = 0 , \quad (4\text{-}20)$$

in which the transient time derivative term is neglected compared to the other terms in the equation. Time enters the equation as a parameter specifying the position of the wetting front $l(t)$. This equation has been considered by Macey (1959) for various forms of the effective diffusion coefficient $\tilde{D}$. For the van Genuchten relations, the effective diffusion coefficient $\tilde{D}$ is given by

$$\tilde{D}(S) = \frac{\alpha\beta\lambda}{K} D(S) = \sqrt{S}\left[1 - \left(1 - S^{1/\lambda}\right)^{\lambda}\right]^2 \left(S^{-1/\lambda} - 1\right)^{-\lambda} S^{-(1+\lambda)/\lambda} . \quad (4\text{-}21)$$

4.2.1 Solution to the Quasi-Stationary State Transport Equations

Integrating Eq. (4-20) leads to the expression

$$\tilde{D}(S)\frac{dS}{dx} = -F_0(t) , \quad (4\text{-}22)$$

where $F_0(t)$ is a (positive) constant of integration, which in this case also depends on the time t. Integrating this equation with respect to distance gives

$$I(S) = \int_{S(x,t)}^{S_0} \tilde{D}(S')dS' = F_0(t)x . \quad (4\text{-}23)$$

It follows that if the liquid saturation vanishes at the wetting front $l(t)$, then

$$I_0 = \int_0^{S_0} \tilde{D}(S)dS = F_0(t)l(t) , \quad (4\text{-}24)$$

or

$$F_0(t) = \frac{I_0}{l(t)} . \quad (4\text{-}25)$$

Equation (4-23) defines the solution to the quasi-stationary state transport equations provided the wetting front position $l(t)$ is known.

A somewhat more elegant alternative approach to solving the quasi-stationary state transport equation is to introduce the variable $y(S)$ defined by

$$y(S) = \int_S^{S_0} D(S')dS' . \quad (4\text{-}26)$$

In terms of y, the transient transport equation becomes

$$\phi\frac{\partial y}{\partial t} = D[S(y)]\frac{\partial^2 y}{\partial x^2} . \quad (4\text{-}27)$$

The advantage of this representation is that the diffusivity is moved out from under the differentiation with respect to distance on the right-hand side of the equation. The quasi-stationary state transport equation is simply:

$$\frac{d^2y}{dx^2} = 0 \,, \tag{4-28}$$

with the immediate solution

$$y = ax + b \,, \tag{4-29}$$

with a and b constants of integration. From the condition $y(0)=0$, it follows that $b=0$. Furthermore,

$$a = \frac{dy}{dx} = D(S)\frac{dS}{dx} \,. \tag{4-30}$$

The next step is to determine the position of the wetting front $l(t)$ by the requirement of global mass conservation.

4.2.2 Global Mass Conservation

The position of the wetting front $l(t)$ in the quasi-stationary state approximation is determined from the transient transport equation by demanding global mass conservation. Returning to the transient mass transport equation, Eq. (4-7), and integrating over the entire spatial domain from $x=0$ to $x=\infty$, yields

$$\frac{d}{dt}\int_0^\infty S(x,t)dx = -\frac{D(S)}{\phi}\frac{dS}{dx}\Big|_{x=0} = \frac{K}{\alpha\beta\lambda}\frac{F_0(t)}{\phi} = \frac{K}{\alpha\beta\lambda}\frac{I_0}{\phi l(t)} \,. \tag{4-31}$$

Writing

$$\frac{dx}{dS} = -\frac{\tilde{D}(S)}{F_0(t)} = -\frac{\tilde{D}(S)}{I_0}l(t) \,, \tag{4-32}$$

by rearranging Eq. (4-22) and using Eq. (4-25), it follows that the left-hand side of the above relation can be expressed alternatively as

$$\frac{d}{dt}\int_{S_0}^{S_r} S\frac{dx}{dS}dS = \frac{M_0}{I_0}\frac{dl(t)}{dt} \,, \tag{4-33}$$

where

$$M_0 = \int_{S_r}^{S_0} S\tilde{D}(S)dS \,. \tag{4-34}$$

Equating the right-hand sides of Eqs. (4-31) and (4-33) yields

$$\frac{dl}{dt} = \frac{2K_0}{l(t)} , \tag{4-35}$$

where

$$K_0 = \frac{I_0^2}{2\phi M_0} \frac{K}{\alpha\beta\lambda} . \tag{4-36}$$

Integrating Eq. (4-35) leads to the following expression for the position of the wetting front

$$l(t) = 2\sqrt{K_0 t} . \tag{4-37}$$

This result holds only for the case in which gravity is absent.

Substituting Eqs. (4-25), (4-36), and (4-37) into Eq. (4-23), the saturation state $S(x,t)$ is then obtained, at any position x and time t, from the integral equation:

$$\int_{S(x,t)}^{S_0} \tilde{D}(S')dS' = \frac{I_0 x}{l(t)} = \frac{I_0 x}{2\sqrt{K_0 t}} = \frac{x}{2}\sqrt{\frac{2\phi M_0}{t}\frac{K}{\alpha\beta\lambda}} . \tag{4-38}$$

In the next section, this relation is evaluated for the case of constant diffusivity for which the exact transient solution is known.

4.2.2.1 Pure Diffusion with Constant Diffusivity

Although the only steady-state solution to the pure diffusion equation with constant diffusivity is an infinite system in a constant concentration profile, nevertheless, the same approach used for the Richards' equation with variable D applies in this case to compute the "diffusion" front. For the case of constant diffusivity, the transport equation becomes

$$\frac{\partial C}{\partial t} = D\frac{\partial^2 C}{\partial x^2} . \tag{4-39}$$

This equation has the exact solution

$$C_{ex}(x,t) = C_0 \operatorname{erfc}\left(\frac{x}{2\sqrt{Dt}}\right) , \tag{4-40}$$

for the initial and boundary conditions

$$C_{ex}(x,0) = 0 , \tag{4-41}$$

and

$$C_{ex}(0,t) = C_0 \,, \tag{4-42}$$

respectively. The quasi-stationary state approximation is given by

$$C_{qss}(x,t) = C_0\left[1 - \frac{x}{l(t)}\right] , \tag{4-43}$$

for $x \le l(t)$, and 0 otherwise. The position of the diffusion front $l(t)$ is given by the equation

$$l(t) = 2\sqrt{Dt} \,. \tag{4-44}$$

The quasi-stationary state approximation is only approximately mass conserving as can be seen by comparing the total mass of liquid in the system obtained at any time t with the exact solution. It follows that for the exact case

$$M_{ex}(t) = \int_0^\infty C_{ex}(x,t)dx = 2C_0\sqrt{\frac{Dt}{\pi}} \,. \tag{4-45}$$

On the other hand, it follows that for the quasi-stationary state approximation

$$M_{qss}(t) = \int_0^\infty C_{qss}(x,t) = C_0\sqrt{Dt} \,. \tag{4-46}$$

Their ratio is given by

$$\frac{M_{ex}}{M_{qss}} = \frac{2}{\sqrt{\pi}} \simeq 1.128 \,, \tag{4-47}$$

and is independent of time.

4.2.2.2 Advection—Diffusion

A similar comparison can be made for the advection-diffusion equation given by

$$\frac{\partial}{\partial t}(\phi C) = \phi D\frac{\partial^2 C}{\partial x^2} - u\frac{\partial C}{\partial x} \,, \tag{4-48}$$

with the initial and boundary conditions:

$$C(0,t) = C_0 \,, \tag{4-49}$$

$$C(x,0) = 0 \ . \tag{4-50}$$

This equation has the well-known exact solution

$$C_{ex}(x,t) = \frac{1}{2} C_0 \left[\mathrm{erfc}\left(\frac{x-ut}{2\sqrt{Dt}} \right) + \exp\left(\frac{ux}{\phi D} \right) \mathrm{erfc}\left(\frac{x+ut}{2\sqrt{Dt}} \right) \right] . \tag{4-51}$$

The quasi-stationary state approximation transport equation is given by

$$\frac{d^2 C_{qss}}{dx^2} - u \frac{dC_{qss}}{dx} = 0 \ , \tag{4-52}$$

with the solution

$$C_{qss}(x,t) = C_0 \frac{1 - \exp\left\{ \frac{u[x - l(t)]}{\phi D} \right\}}{1 - \exp\left[- \frac{ul(t)}{\phi D} \right]} \ . \tag{4-53}$$

From the requirement of mass conservation the wetting front $l(t)$ can be shown to obey the integral equation

$$\int_0^{l(t)} dl' \left[1 - \frac{ul'}{\phi D} \frac{1}{e^{ul'/(\phi D)} - 1} \right] = \frac{ut}{\phi} \ . \tag{4-54}$$

For large t [and $l(t)$], the second term in the integral can be neglected and the front is given by

$$l(t) \sim vt \ . \tag{4-55}$$

In the exact case, conservation of total mass yields the expression

$$M_{ex}(t) = \int_0^{\infty} C(x,t)dx,$$

$$= \frac{C_0}{2}\left\{ vt\left[1 + \text{erf}\left(\frac{v}{2}\sqrt{\frac{t}{D}}\right)\right] + 2\sqrt{\frac{Dt}{\pi}}\exp\left(-\frac{v^2t}{4D}\right)\right. \tag{4-56}$$

$$\left. + \frac{2D}{v}\text{erf}\left(\frac{v}{2}\sqrt{\frac{t}{D}}\right)\right\}.$$

In the limit $t \to \infty$, it follows that asymptotically

$$\lim_{t\to\infty} M_{ex}(t) = C_0 vt\ . \tag{4-57}$$

By contrast, the quasi-stationary state approximation yields the result

$$M_{qss}(t) = \int_0^{l(t)} C_{qss}(x,t)dx$$

$$= C_0\left\{\frac{l(t)}{1 - \exp\left[-vl(t)/D\right]} - \frac{D}{v}\right\} - C_0 l(t)\ . \tag{4-58}$$

Therefore, for sufficiently long times, the exact result and quasi-stationary state approximation agree.

4.3 NUMERICAL RESULTS

In this section, a numerical example is presented describing propagation of a wetting front migrating into a porous medium with an initial saturation of 10 percent. Comparison is made between the quasi-stationary state approximation and the transient solution for fixed and adaptive grids. These results are compared with the Philip solution (Philip, 1955). The adaptive grid algorithm used in the calculations is described in the appendix.

The finite difference form of Richards' equation, Eq. (4-4), for variable grid spacing is written as the fully backward form:

$$\phi\frac{S_n^{k+1} - S_n^k}{\Delta t} - K\frac{k^r_{n+1/2}\dfrac{h_{n+1}^{k+1} - h_n^{k+1}}{\Delta x_n} - k^r_{n-1/2}\dfrac{h_n^{k+1} - h_{n-1}^{k+1}}{\nabla x_n}}{\delta x_n} = 0\ , \tag{4-59}$$

for the $k + 1$ time step, with the finite difference grid defined by the nodal points (x_n), $n = 0, \ldots, N$, with $x_0 = 0$ and $x_N = L$ with L the total length of the system. The operators Δ, ∇, and δ are defined by:

$$\Delta x_n = x_{n+1} - x_n \,, \tag{4-60}$$

$$\nabla x_n = x_n - x_{n-1} \,,$$

$$\delta x_n = x_{n+\frac{1}{2}} - x_{n-\frac{1}{2}} \,,$$

$$= \frac{1}{2}\left(x_{n+1} - x_{n-1}\right) \,,$$

$$= \frac{1}{2}\left(\Delta x_n + \nabla x_n\right) \,. \tag{4-61}$$

For equal node spacing Δx, it follows that

$$\Delta x_n = \nabla x_n = \delta x_n = \Delta x \,. \tag{4-62}$$

This form of the finite difference equation is mass conserving. Thus,

$$\sum_n \left(\delta_n^{k+1} - S_n^k\right) \delta x_n = \frac{\Delta t}{\phi}\left(F_1 - F_{N+1}\right) \,, \tag{4-63}$$

where F_1 and F_{N+1} denote the flux into and out of the system, respectively.

Figure 4-1 shows the liquid saturation profile of a wetting front plotted as a function of distance for an elapsed time of 1 yr as predicted by the quasi-stationary state approximation, adaptive and fixed grid finite difference solutions, and the exact Philip solution. As can be seen from the figure, the adaptive grid solution gives much better agreement compared to the fixed grid solution with the Philip solution. The quasi-stationary state approximation is seen to underestimate the wetting profile. The applicability of the quasi-stationary state approximation could be improved by adding a boundary layer solution following the work of Zimmerman and Bodvarsson (1990).

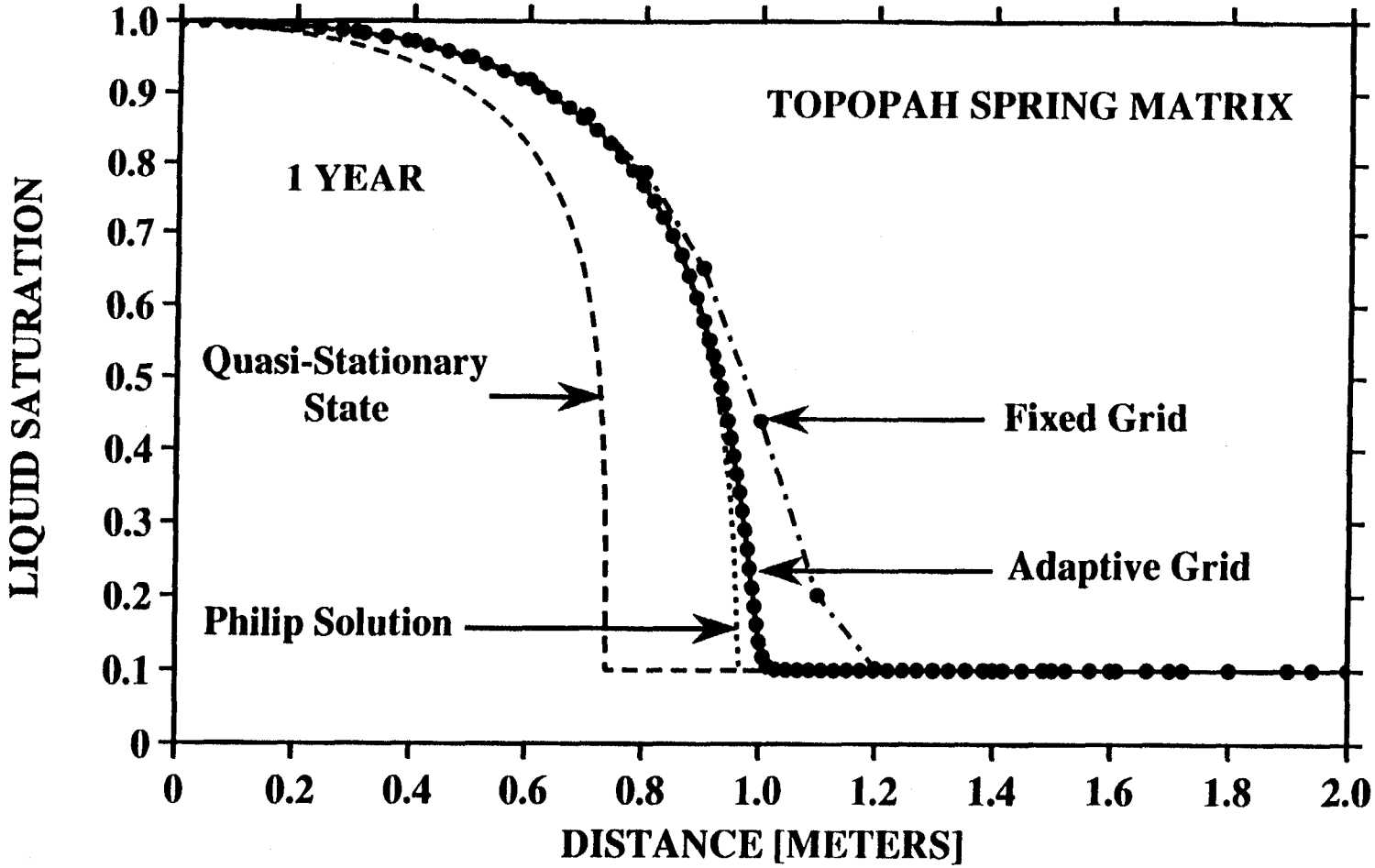

Figure 4-1. Comparison of the quasi-stationary state approximation with transient solutions based on fixed and variable grids for a wetting front propagating into a partially saturated porous medium with an initial saturation of 10 percent. Also shown is the Philip solution. Circles give the positions of the node points used in the calculations for adaptive and fixed grids, respectively. van Genuchten parameters corresponding to the Yucca Mountain Topopah Spring matrix were used in the calculations.

5 STEADY-STATE HEAT-PIPE

Of special importance in the near-field region of a HLW repository is the possible formation of heat-pipes, a thermalhydrologic process in which counterflow of liquid and vapor occurs. At the hot end of the heat-pipe evaporation of liquid takes place, which condenses at the cold end located some distance away. Recharge of liquid to the hot end of the pipe may occur by gravity or capillary forces. Because the evaporation process leaves behind dissolved salts, the heat-pipe could be an important mechanism for increasing the concentration of aqueous solutions present in the near-field after the repository has cooled sufficiently for liquid water to become stable.

5.1 GRAVITY—NO CAPILLARY FORCES

Within the heat-pipe region, the temperature-pressure variation with depth is constrained by the saturation curve of water separating liquid and vapor phases:

$$T(x) = T_{sat}\left[p_l(x)\right] . \tag{5-1}$$

The behavior of pressure with depth follows from the steady-state mass and heat transport equations for the heat-pipe (Turcotte and Schubert, 1982). Under steady-state conditions, mass conservation is described by

$$F_l + F_g = \rho_l q_l + \rho_g q_g = 0, \tag{5-2}$$

and energy conservation by

$$h_l \rho_l q_l + h_g \rho_g q_g = H, \tag{5-3}$$

where H, a negative quantity if the vertical axis is taken as positive pointing downwards, denotes the heat entering the heat-pipe from below. The Darcy flux of liquid water and water vapor are given by

$$q_l = -\frac{k k_l}{\mu_l}\left(\frac{dp}{dx} - \rho_l g\right), \tag{5-4}$$

$$q_g = -\frac{k k_g}{\mu_g}\left(\frac{dp}{dx} - \rho_g g\right), \tag{5-5}$$

where the relative permeabilities are functions of saturation. Assuming they depend linearly on saturation yields

$$k_l = S_l, \tag{5-6}$$

$$k_g = S_g = 1 - S_l, \tag{5-7}$$

assuming that

$$k_l + k_g = 1. \tag{5-8}$$

These equations provide two independent equations in the two unknowns dp/dx and S_l.

The energy conservation equation can be expressed in terms of the latent heat L according to

$$H = -\rho_l q_l L = \rho_g q_g L, \tag{5-9}$$

where

$$L = h_g - h_l = h_{gl}, \tag{5-10}$$

by making use of the mass conservation equation. The Darcy flux for liquid and vapor then becomes:

$$q_l = -\frac{H}{\rho_l L}, \tag{5-11}$$

and

$$q_g = \frac{H}{\rho_g L}. \tag{5-12}$$

It follows that the pressure gradient can be expressed in the form:

$$\frac{dp}{dx} = \frac{\dfrac{k_l \rho_l^2}{\mu_l} + \dfrac{k_g \rho_g^2}{\mu_g}}{\dfrac{k_l \rho_l}{\mu_l} + \dfrac{k_g \rho_g}{\mu_g}} g, \tag{5-13}$$

from which the heat flux can be determined as

$$H = -\frac{L k k_g k_l \rho_g \rho_l}{\mu_l \mu_g} \left(\frac{\rho_l - \rho_g}{\dfrac{k_l \rho_l}{\mu_l} + \dfrac{k_g \rho_g}{\mu_g}} \right). \tag{5-14}$$

As noted by Turcotte and Schubert (1982), for a given permeability a maximum heat flux exists above which burnout of the heat-pipe occurs. The maximum value occurs at a liquid saturation of

$$S_l^{max} = \frac{\sqrt{\frac{\mu_l \rho_g}{\rho_l \mu_g}} - \frac{\mu_l \rho_g}{\rho_l \mu_g}}{1 - \frac{\mu_l \rho_g}{\rho_l \mu_g}}, \tag{5-15}$$

at a maximum heat flow rate expressed in terms of the dimensionless quantity Γ of

$$\Gamma_{max} = \left(1 + \sqrt{\frac{\mu_l \rho_g}{\rho_l \mu_g}}\right)^{-2}, \tag{5-16}$$

where

$$\Gamma = \frac{H \mu_g}{kLg\rho_g(\rho_g - \rho_l)}. \tag{5-17}$$

Equating H with the heat produced from a waste canister allows the mininum permeability to be computed below which burnout of the heat-pipe would occur. For example, for boiling of water at atmospheric pressure taking the values $\mu_g = 1.25 \times 10^{-5}$ Pa·s, $\mu_l = 2.84 \times 10^{-4}$ Pa·s, $\rho_g = 0.598$ kg·m^{-3}, $\rho_l = 10^3$ kg·m^{-3}, $L = 2500 \times 10^3$ J·kg^{-1}, and $g = 9.8$ m·s^{-2}, burnout occurs at permeabilities below approximately 10^{-14} m^2 for a heat flux of 10 W·m^{-2}.

In a HLW repository, for a heat generation rate of 114 kw/acre the corresponding heat-pipe burnout permeability is approximately 10^{-12} m^2. It should be noted, however, that for a partially saturated porous medium, capillary forces are expected to dominate over gravity (Udell, 1983).

5.2 GRAVITY AND CAPILLARY FORCES

In addition to gravity, the recharge of liquid water can also occur due to capillary effects. This type of heat pipe has been studied extensively for partially saturated media (Udell, 1983, 1985; Doughty and Pruess, 1988, 1990) and includes an air component (Doughty and Pruess, 1992). The results are only briefly summarized here. Incorporating capillary forces leads to the Darcy flux of liquid water and water vapor given by

$$q_l = -\frac{kk_l}{\mu_l}\left(\frac{dp_l}{dx} - \rho_l g\right), \tag{5-18}$$

$$q_g = -\frac{kk_g}{\mu_g}\left(\frac{dp_g}{dx} - \rho_g g\right), \tag{5-19}$$

with different pressures p_l and p_g for the liquid and gas phases, respectively. They are related by the capillary pressure p_c, according to the equation

$$p_g - p_l = p_c \,. \tag{5-20}$$

From conservation of mass and energy it follows that

$$\frac{dp_l}{dx} = \frac{\mu_l H}{\rho_l k k_l L} + \rho_l g \,, \tag{5-21}$$

and

$$\frac{dp_g}{dx} = -\frac{\mu_g H}{\rho_g k k_g L} + \rho_g g \,. \tag{5-22}$$

The gradient of the capillary pressure can be expressed as

$$\frac{dp_c}{dx} = -\frac{H}{kL}\left(\frac{\mu_l}{\rho_l k_l} + \frac{\mu_g}{\rho_g k_g}\right) - (\rho_l - \rho_g)g \,. \tag{5-23}$$

From this equation, the liquid saturation profile within the heat-pipe region can be obtained by expressing p_c in terms of S_l. It follows for a given functional relation

$$p_c = p_c(S_l) \,, \tag{5-24}$$

that

$$\frac{dp_c}{dx} = \frac{dp_c}{dS_l}\frac{dS_l}{dx} \,. \tag{5-25}$$

Consequently, the liquid saturation profile within the two-phase heat-pipe zone can be expressed in terms of the integral

$$\int_{S_r}^{S_l(x)} \frac{1}{\frac{H}{kL}\left(\frac{\mu_l}{\rho_l k_l} + \frac{\mu_g}{\rho_g k_g}\right) + (\rho_l - \rho_g)g} \frac{dp_c}{dS_l} dS_l = -x \,. \tag{5-26}$$

The temperature profile is obtained from the Kelvin equation for vapor pressure lowering given by

$$p_l = p_{sat} e^{\frac{p_c}{\rho_l RT}} \,, \tag{5-27}$$

combined with the Clasius-Clapeyron equation

$$\frac{dp}{dT} = \frac{\Delta S}{\Delta V} = \frac{\Delta H}{T}\frac{p}{RT}, \tag{5-28}$$

which gives

$$p_{sat} = p_0 \exp\left[-\left(\frac{1}{T} - \frac{1}{T_0}\right)\frac{L}{R}\right], \tag{5-29}$$

with $L = \Delta H$. Consequently the temperature in the heat-pipe region is given by

$$T(x) = \frac{T_0\left(1 + \frac{p_c}{L\rho_l}\right)}{1 - \frac{RT_0}{L}\ln\frac{p_g}{p_l}}. \tag{5-30}$$

6 ESTIMATING CHANGES IN POROSITY AND PERMEABILITY

In this section, an attempt is made to estimate the maximum increase in porosity and permeability that could occur in a system with refluxing fluid that is well-undersaturated chemically with respect to the host rock minerals. This undersaturation could occur at the condensation region of a stationary heat-pipe, for example. However, for these results to apply, the heat-pipe would have to remain stationary for a relatively long time period of hundreds to several thousands of years, which is unlikely. The calculations presented here do not take into account the possible formation of secondary mineral products that could reduce the porosity and permeability.

To compute changes in porosity and permeability, it is necessary to calculate the rate at which the minerals dissolve at the desired temperature, which in this exercise is assumed to be 100 °C, the maximum temperature that can occur in a partially saturated porous medium at 1-bar pressure. Note, however, that vapor pressure lowering due to capillary forces could result in substantially higher temperatures. The mineral dissolution rate involves the kinetic rate constant, mineral surface area, and chemical saturation state of the mineral in the aqueous solution in which it is reacting. The kinetic rate constant is given as a function of temperature by the equation

$$k(T) = k_0 \frac{T}{T_0} e^{-\frac{\Delta H}{R}\left(\frac{1}{T}-\frac{1}{T_0}\right)}, \qquad (6\text{-}1)$$

where k_0 denotes the rate constant at temperature $T_0 = 25$ °C, ΔH is the enthalpy of activation, and R denotes the gas constant. The rate constants of K-feldspar and cristobalite are plotted in Figure 6-1 as a function of temperature using activation enthalpies of 35.3 and 75.3 kJ mol^{-1}, and rate constants of 3×10^{-16} and 1.58×10^{-18} mol cm^{-2} sec^{-1}, respectively. The rate constant for cristobalite is derived from data of Rimstidt and Barnes (1980) and the K-feldspar data from Helgeson et al. (1984). As can be seen from the figure, the K-feldspar rate constant increases by approximately 1.3 and cristobalite by 2.75 log units from 25 to 100 °C.

The maximum change in porosity and permeability can be calculated independently of the fluid flow velocity by allowing the minerals in the rock to dissolve at the far from equilibrium dissolution rate. It must be emphasized that this gives the maximum change possible for a given rate constant, and ignores effects of the chemical saturation state on the dissolution rate, which would act to reduce the rate or even change its sign. To calculate the dissolution rate, it is necessary to make some assumption regarding the change in surface area with reaction progress. Fortunately, the final results should not differ greatly (less than an order of magnitude) for different assumptions made. Clearly in the limit that a mineral grain completely dissolves, the surface area must vanish. One possible form for the variation of mineral surface area with dissolution is to assume a two-thirds dependence of the surface area on mineral volume fraction according to the expression:

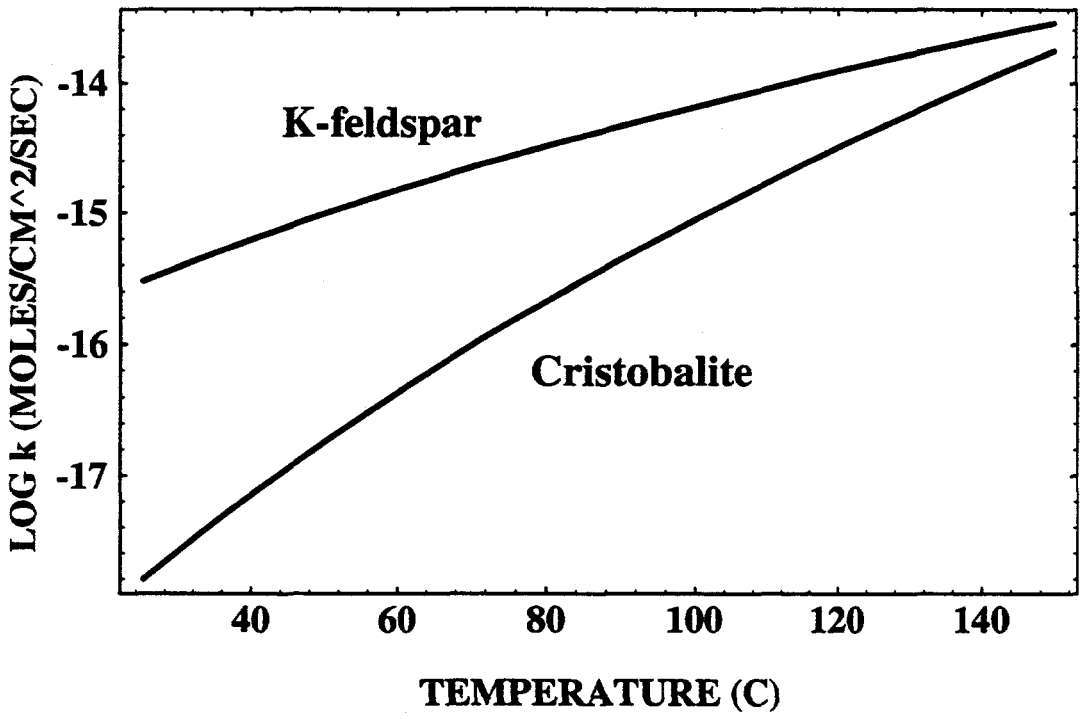

Figure 6-1. Rate constants for K-feldspar and cristobalite plotted as a function of temperature

$$s_m = s_m^0 \left(\frac{\phi_m}{\phi_m^0} \right)^{2/3} , \tag{6-2}$$

where s_m^0 and ϕ_m^0 denote the initial surface area and volume fraction of the mth mineral. The initial surface area taken to be proportional to the amount of the mth mineral present and inversely proportional to the mineral grain size b_m, is as follows

$$s_m^0 = \phi_m^0 \frac{6}{b_m} , \tag{6-3}$$

where the factor 6 arises from the 6 faces of a cube. For far from equilibrium conditions, the change in mineral volume fraction at a fixed point in space satisfies the differential equation

$$\frac{\partial \phi_m}{\partial t} = -\bar{V}_m k_m s_m^0 \left(\frac{\phi_m}{\phi_m^0} \right)^{2/3} , \tag{6-4}$$

where $\bar{V}_m$ denotes the mineral molar volume. This equation has the solution (Helgeson et al., 1984)

$$\phi_m(t) = \phi_m^0 \left(1 - \frac{1}{3} \frac{\bar{V}_m k_m s_m^0}{\phi_m^0} t \right)^3 . \tag{6-5}$$

The mineral completely dissolves when

$$t = 3 \frac{\phi_m^0}{\bar{V}_m k_m s_m^0} . \tag{6-6}$$

The time for the mineral volume fraction to change by a factor ϵ denoted by t_ϵ, is given by

$$t_\epsilon = \frac{3\phi_m^0}{\bar{V}_m k_m s_m^0} (1 - \epsilon^{1/3}) . \tag{6-7}$$

The quantity t_ϵ is plotted in Figure 6-2 as a function of temperature for K-feldspar and cristobalite for $\epsilon = 0.9$, that is, a 10-percent change in mineral volume fraction, using $\phi_{Kf}^0 = 0.6$, $\phi_{Cb}^0 = 0.3$, and $s_{Kf}^0 = 36{,}000$, $s_{Cb}^0 = 18{,}000$ cm^{-1}, that is, one-tenth of a millimeter-sized grain ($\bar{V}_{Cb} = 25.74$, $\bar{V}_{Kf} = 108.9$ cm^3 mol^{-1}). These values are representative of tuff at YM. With these values at 100 °C, cristobalite takes approximately 2,400 yr and K-feldspar only 75 yr for the volume fraction to change by 10 percent, both well within the time span that a temperature of this magnitude can be maintained in a HLW repository.

It should be kept in mind that the rate constants and surface areas may be uncertain by orders of magnitude. It has been observed, for example, that the rate of quartz dissolution can increase by orders of magnitude with the addition of alkali to the solution (Dove and Crerar, 1990). Therefore the value used here for cristobalite may be too small, and hence the time for a 10 percent change in volume fraction too long. However, the measured groundwaters at YM are supersaturated with respect to cristobalite indicating the presence of a kinetic barrier at 25 °C. Furthermore, it has been tacitly assumed that water is able to come in contact with the entire surface of a mineral grain. This assumption may be unrealistic, and water may contact only a tiny fraction of any given grain.

The change in permeability can be estimated from a phenomenological equation of the form

$$\kappa = \kappa_0 \left(\frac{\phi}{\phi_0} \right)^\sigma , \tag{6-8}$$

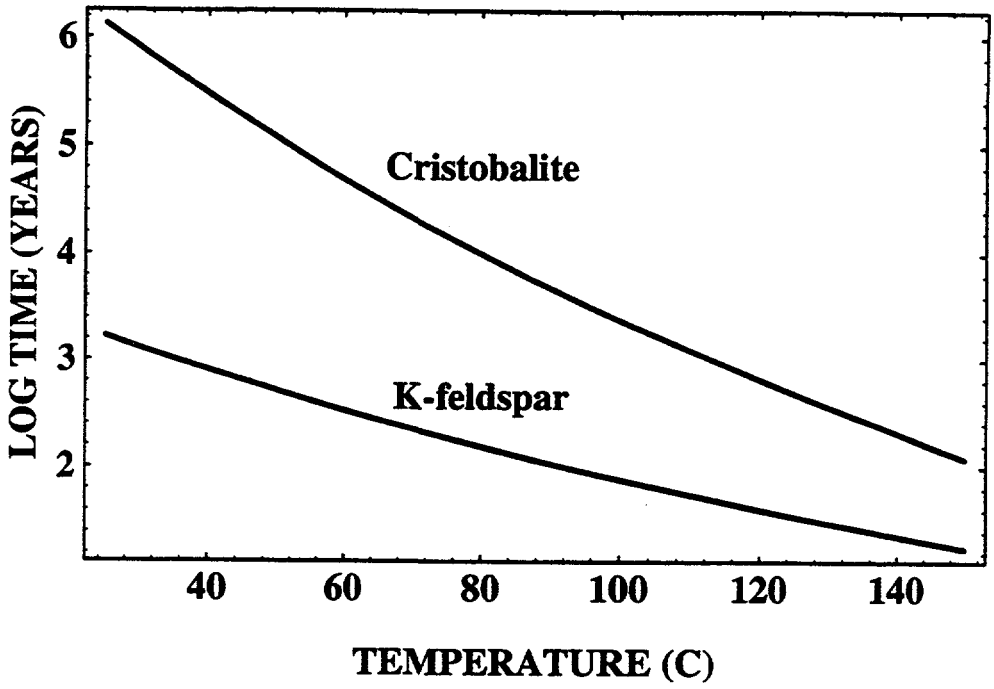

Figure 6-2. Time required for the volume fractions of K-feldspar and cristobalite to change by 10 percent plotted as a function of temperature from Eq. (6-7). See text for values of parameters used in the calculation.

where κ_0 denotes the initial permeability of the porous medium. This equation represents the permeability as the porosity raised to some power σ. It gives the correct limiting value of the permeability of zero for zero porosity. But it does not account for the change in permeability resulting from the change in mineral texture, for example. If the porosity is related to the mineral volume fractions by the usual equation

$$\phi = 1 - \sum_m \phi_m \,, \tag{6-9}$$

which leads to the expression

$$\kappa = \kappa_0 \left(\frac{1 - \sum_m \phi_m}{1 - \sum_m \phi_m^0} \right)^{\sigma} . \tag{6-10}$$

The volume fractions of K-feldspar and cristobalite are plotted in Figure 6-3 as a function of temperature for an elapsed time of 1,000 yr. K-feldspar is the first mineral to completely dissolve. The ratio κ/κ_0 is plotted as a function of temperature in Figure 6-4 for different times of 100, 1,000, and 10,000 yr for a rock composed of 60 percent K-feldspar and 30 percent cristobalite with a porosity of 10 percent using the rates and surface areas given above.

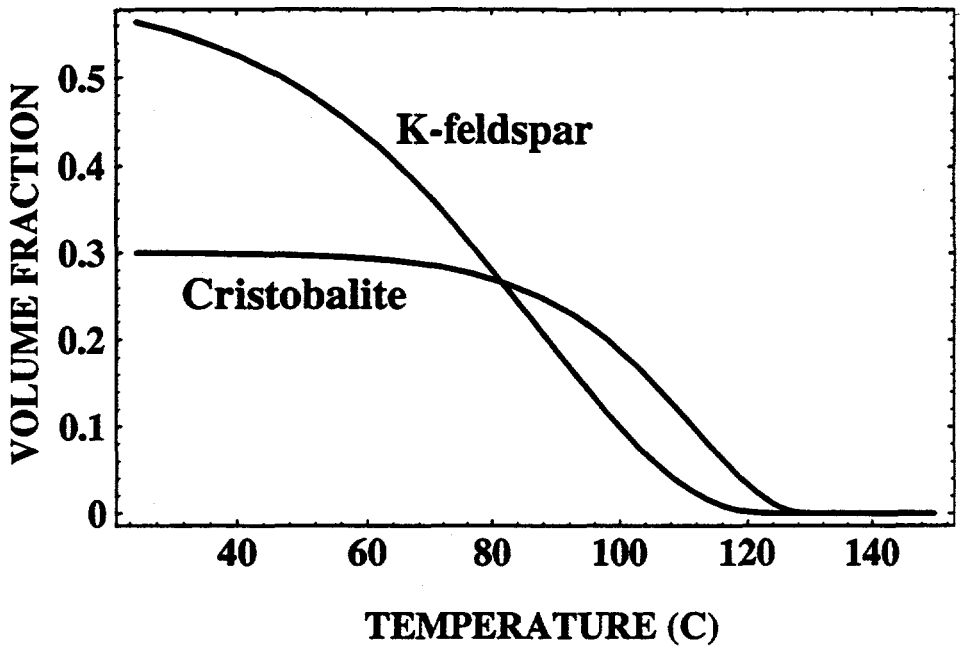

Figure 6-3. Volume fractions of K-feldspar and cristobalite for a tuffaceous rock initially composed of 60-percent K-feldspar 30-percent cristobalite plotted as a function of temperature for an elapsed time of 1,000 yr. The same values for the kinetic rate constants, surface areas are used as in Figure 6-2.

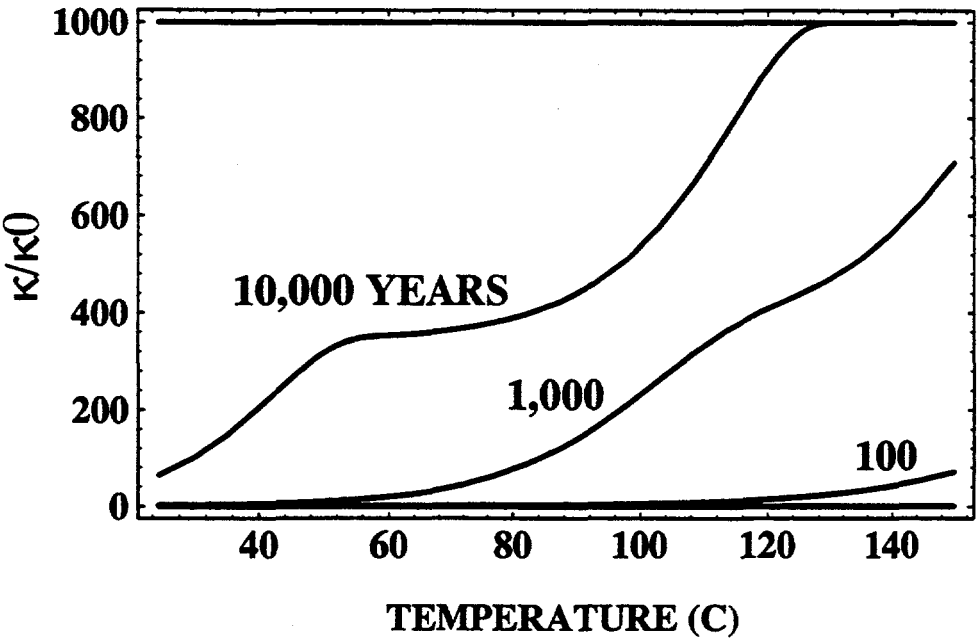

Figure 6-4. Changes in permeability κ/κ_0 for a rock composed of 60-percent K-feldspar and 30-percent cristobalite plotted as a function of temperature for times of 100, 1,000, and 10,000 yr with $\alpha=3$. The same values for values for the kinetic rate constants and surface areas are used as in Figure 6-2.

The plateau in the permeability curves occurs when K-feldspar completely dissolves. Note that the largest possible increase in permeability occurs when the porosity is unity, which gives the result

$$\kappa_{max} = \kappa_0 \phi_0^{-\sigma} \quad . \tag{6-11}$$

For $\phi_0 = 0.1$ and $\sigma = 3$, $\kappa_{max}/\kappa_0 = 1{,}000$, consistent with the figure.

7 SUMMARY

Mass and energy conservation equations were formulated for multiphase-multicomponent transport in a partially saturated porous medium. Included in the description were chemical reactions involving mineral precipitation-dissolution reactions, aqueous complexing, ion pairing, dissociation of water, and adsorption and ion-exchange. The DGM for transport of gases in low-permeable rocks characterized by molecular mean free paths comparable to or longer than typical pore size dimensions was reviewed. Explicit expressions were derived for the segregative and nonsegregative components of the diffusive flux. Richards' equation was solved for both the transient and the quasi-stationary state solution, and the results were compared for a wetting front imbibing into an unsaturated tuffaceous rock matrix using parameters characteristic of the Topopah Spring member of YM. It was found that the position of the wetting front as predicted by the quasi-stationary state approximation, lagged behind the solution to the full transient equations. Burnout permeabilities for a 1D heat pipe were estimated for gravity driven reflux of liquid. Finally an estimate was presented for the change in porosity and permeability resulting from reaction of a dilute aqueous solution with YM tuff at elevated temperatures. Significant changes were possible in time spans of thousands of years or less.

8 REFERENCES

Ali S.M., F.G. King, and S. Ilias. 1994. Diffusive transport of carbon dioxide through USW-G4 Topopah Spring tuffs. *Scientific Basis for Nuclear Waste Management*. Pittsburgh, PA: Materials Research Society.

Bird, R.B., W.E. Stewart, and E.N. Lightfoot. 1960. *Transport Phenomena*. New York, NY: John Wiley & Sons.

Buscheck, T.A., and J.J. Nitao. 1993. The analysis of repository-heat-driven hydrothermal flow at Yucca Mountain. *Proceedings of the Fourth Annual International High-Level Radioactive Waste Management Conference*. La Grange Park, IL: American Nuclear Society: 1: 847–867.

Cunningham, R.E., and R.J.J. Williams. 1980. *Diffusion in Gases and Porous Media*. New York, NY: Plenum Press.

Doughty, C., and K. Pruess. 1988. A semianalytical solution for heat-pipe effects near high-level nuclear waste packages buried in partially saturated geological media. *International Journal of Heat Mass Transfer* 31: 79–90.

Doughty, C., and K. Pruess. 1990. A similarity solution for two-phase water for two-phase fluid and heat flow near high-level nuclear waste packages emplaced in porous media. *International Journal of Heat Mass Transfer* 33: 1,205–1,222.

Doughty, C., and K. Pruess. 1992. A similarity solution for two-phase water, air and heat flow near a linear heat source in a porous medium. *Journal of Geophysical Research* 97: 1,821–1,838.

Dove, P.M., and D.A. Crerar. 1990. Kinetics of quartz dissolution in electrolyte solutions using a hydrothermal mixed flow reactor. *Geochimica et Cosmochimica Acta* 54: 955–969.

Gunn, R.D., and C.J. King. 1969. Mass transport in porous materials under combined gradients of composition and pressure. *AIChE Journal* 15: 507–514.

Helgeson, H.C., W.M. Murphy, and P. Aagaard. 1984. Thermodynamic and kinetic constraints on reaction rates among minerals and aqueous solutions. II. Rate constants, effective surface area, and the hydrolysis of feldspar. *Geochemica Cosmochemica Acta* 48: 2,405–2,432.

Lichtner, P.C. 1985. Continuum model for simultaneous chemical reactions and mass transport in hydrothermal systems. *Geochemica Cosmochemica Acta* 49: 779–800.

Macey, R.I. 1959. A quasi-steady-state approximation method for diffusion problems, 1, Concentration dependent diffusion coefficients. *Bulletin of Mathematical Biophysics* 21: 19–21.

Mason, E.A., and A.P. Malinauskas. 1983. *Gas Transport in Porous Media: The Dusty Gas Model*. Amsterdam, The Netherlands: Elsevier: 194 pp.

Mason, E.A., A.P. Malinauskas, and R.B. Evans III. 1967. Flow and diffusion of gases in porous media. *Journal of Chemical Physics* 46: 3,199-3,216.

Nield, D.A., and A. Bejan. 1992. *Convection in Porous Media.* Springer-Verlag. 408 pp.

Nitao, J.J. 1988. *Numerical Modeling of the Thermal and Hydrological Environment Around a Nuclear Waste Package Using the Equivalent Continuum Approximation: Horizontal Emplacement.* UCID-21444. Livermore, CA: Lawrence Livermore National Laboratory.

Nitao, J.J. 1990. *V-TOUGH—An Enhanced Version of the TOUGH Code for the Thermal and Hydrologic Simulation of Large-Scale Problems in Nuclear Waste Isolation.* UCID- 21954. Livermore, CA: Lawrence Livermore National Laboratory.

Nuclear Regulatory Commission. 1992. Disposal of high-level radioactive wastes in geologic repositories. *Code of Federal Regulations, Title 10, Energy, Part 60 (10 CFR Part 60).* Washington, DC: Office of the Federal Register, National Archives and Records Administration: 91-124.

Oelkers, E.H., and H.C. Helgeson. 1988. Calculation of the thermodynamic and transport properties of aqueous species at high pressures and temperatures. Aqueous tracer diffusion cofficients of ions to 1000 °C and 5 kb. *Geochemica et Cosmochinica Acta* 52: 63-85.

Peters, R.R., E.A. Klavetter, I.J. Hall, S.C. Blair, P.R. Heller, and G.W. Gee. 1984. *Fracture and Matrix Hydrologic Characteristics of Tuffaceous Materials from Yucca Mountain, Nye County, Nevada.* SAND84-1471. Albuquerque, NM: Sandia National Laboratories.

Philip, J.R. 1955. Numerical solution of equations of the diffusive type with diffusivity concentration dependent. *Transactions Faraday Society* 51: 885-892.

Press, W.H., B.P. Flannery, S.A. Terkolsky, and W.T. Vetterling. 1987. *Numerical Recipes.* Cambridge University Press: 818.

Pruess, K. 1987. *TOUGH User's Guide.* LBL-20700. Berkeley, CA: Lawrence Berkeley Laboratory Report.

Pruess, K., C. Calore, R. Celati, and Y.S. Wu. 1987. An analytical solution for heat transfer at a boiling front moving through a porous medium. *International Journal of Heat Mass Transfer* 30: 2,595-2,602.

Rimstidt, J.D., and H.L. Barnes. 1980. The kinetics of silica-water reactions. *Geochimica et Cosmochimica Acta* 44: 1,683-1,699.

Runchal, A.K., and B. Sagar. 1992. *PORFLOW: A Multifluid Multiphase Model for Simulating Flow, Heat Transfer, and Mass Transport in Fractured Porous Media. User's Manual—Version 2.41.* CNWRA 92-003. San Antonio, TX: Center for Nuclear Waste Regulatory Analyses.

Thorstenson, D.C., and D.W. Pollock. 1989a. Gas transport in unsaturated porous media: The adequacy of Fick's law. *Water Resources Research* 25: 477-507.

Thorstenson, D.C., and D.W. Pollock. 1989b. Gas transport in unsaturated zones: Multicomponent systems and the adequacy of Fick's law. *Reviews of Geophysics* 27: 61–78.

Turcotte, D.L., and G. Schubert. 1982. *Geodynamics: Applications of Continuum Physics to Geological Problems.* New York, NY: John Wiley & Sons.

U.S. Environmental Protection Agency. 1992. Environmental radiation protection standards for management and disposal of spent nuclear fuel, high-level and transuranic radioactive wastes. *Code of Federal Regulations, Title 40, Protection of Environment, Part 191 (40 CFR Part 191).* Washington, DC: Office of the Federal Register, National Archives and Records Administration: 7–16.

Ünal, A. 1987. Gaseous mass transport in porous media through a stagnant gas. *Industrial Engineering Chemical Research* 26: 72–77.

Udell, K.S. 1983. Heat transfer in porous media heated from above with evaporation, condensation, and capillary effects. *Journal of Heat Transfer* 105: 485–492.

Udell, K.S. 1985. Heat transfer in porous media considering phase change and capillarity—The heat pipe effect. *International Journal of Heat Mass Transfer* 28: 485–495.

Vincenti, W.G., and C.H. Kruger, Jr. 1965. *Introduction to Physical Gas Dynamics.* Krieger. 538 pp.

Zimmerman, R.W. and G.S. Bodvarsson. 1990. Absorption of water into porous blocks of various shapes and sizes. *Water Resources Research* 26: 2,797–2,805.

APPENDIX
ADAPTIVE GRID

ADAPTIVE GRID

To solve the finite difference equations representing advective, diffusive and dispersive mass transport in the presence of mineral reactions, it is may be necessary to include an adaptive grid to track sharp reaction fronts. For a given concentration profile $C(x)$ of some species, the problem is to obtain a distribution of grid points that are "best" adapted to the profile. One equation for determining the adaptive grid is given by the differential equation (Press et al., 1987, p. 608-611)

$$\frac{dx}{dq} = \frac{\chi_0}{G[x(q)]} , \tag{A-1}$$

where $x(q)$ denotes the position of the qth grid point, with $q=1,\ldots, N$, and the constant χ_0 is fixed by the normalization condition

$$\chi_0 = \frac{1}{N}\int_0^L G(x)dx , \tag{A-2}$$

where L refers to the length of the system. The function $G(x)$ is referred to as the grid-weighting function and controls the density of grid points over the length of the system. The normalization condition ensures that the grid points are distributed over the full length L. A geometrical interpretation of the weight function can be obtained by noting that the area under the $G(x)$ curve between any two neighboring grid points is constant

$$\int_{x_{q-1}}^{x_q} G(x)dx = \chi_0 . \tag{A-3}$$

Thus, the smaller $G(x)$ throughout an interval, the greater is the grid spacing.

There are many possible prescriptions for $G(x)$. Several expressions are given below. One involves the logarithmic derivative of the function C:

$$G(x) = \frac{1}{\Delta} + \frac{1}{\delta}\left|\frac{d \ln C}{dx}\right|^a . \tag{A-4}$$

The quantity Δ gives the background density of grid points and δ controls their distribution for a given function $C(x)$. The quantity a is a positive exponent usually taken less than one. It follows that

$$\chi_0 = \frac{L}{N\Delta} + \frac{1}{\delta}\int_0^L \left|\frac{d \ln C}{dx}\right|^a dx = 1 + \frac{1}{\delta}\int_0^L \left|\frac{d \ln C}{dx}\right|^a dx , \tag{A-5}$$

assuming

$$\Delta = \frac{L}{N} . \tag{A-6}$$

Another possibility involves the first, second, or higher derivatives of C, for example Therefore, $\chi_0 \geq 1$.

$$G_\alpha(x) = \sqrt{\frac{1}{\Delta^2} + \frac{1}{\delta}\left(\frac{d^\alpha C}{dx^\alpha}\right)^2} , \tag{A-7}$$

or a combination thereof

$$G_\alpha(x) = \sqrt{\frac{1}{\Delta^2} + \frac{1}{\delta_1}\left(\frac{dC}{dx}\right)^2 + \frac{1}{\delta_2}\left(\frac{d^2C}{dx^2}\right)^2} . \tag{A-8}$$

A.1 NUMERICAL IMPLEMENTATION

Integrating the differential equation Eq. (A-1) for the adaptive grid location yields an integral equation for determining the position of the adaptive grid point $x(q)$:

$$\int_0^{x_q} G(x)\,dx = \frac{q}{N}\int_0^L G(x)\,dx . \tag{A-9}$$

To implement the adaptive gridding algorithm numerically, note that $C(x)$ is known only approximately and therefore also $G(x)$ and χ_0. The scale factor χ_0 is determined by numerically integrating the gridding function over the x-axis:

$$\chi_0 = \frac{1}{N}\int_0^L G(x)\,dx \approx \frac{1}{2N}\sum_{n=1}^{N}\left(G_n + G_{n-1}\right)\left(x_n - x_{n-1}\right) . \tag{A-10}$$

To evaluate the integral on the left-hand side of Eq. (A-9), note that it may be expressed in the form:

$$\int_0^{x(q)} G(x)\,dx = W_n + \int_{x_n}^{x(q)} G(x)\,dx , \tag{A-11}$$

where W_n denotes the partial sum over the gridding function

$$W_n = \int_0^{x_n} G(x)dx \simeq \frac{1}{2}\sum_{l=1}^{n} \left(G_l + G_{l-1}\right)\left(x_l - x_{l-1}\right) , \tag{A-12}$$

and where $x(q)$ satisfies the inequality:

$$x_n \le x(q) \le x_{n+1} .$$

The coordinate x_n is determined by the requirement that

$$W_{n+1} = \int_0^{x_{n+1}} G(x)dx > q\chi_0 , \tag{A-14}$$

a necessary and sufficient condition for Eq. (A-13) to hold.

The integral appearing in the second term on the right-hand side of Eq. (A-11) may be evaluated by linearly interpolating the function G. Writing

$$\int_{x_n}^{x(q)} G(x)dx = \frac{1}{2}\left\{G(x_n) + G\left[x(q)\right]\right\}\left[x(q) - x_n\right] , \tag{A-15}$$

and interpolating to obtain the value for $G[x(q)]$ according to the expression

$$G[x(q)] \simeq G(x_n) + \frac{G_{n+1} - G_n}{x_{n+1} - x_n}\left[x(q) - x_n\right] , \tag{A-16}$$

yields the following quadratic expression for the adapted grid point $x(q)$:

$$x(q) = x_n + \frac{1}{2A}\left(-B + \sqrt{B^2 - 4AC}\right) , \tag{A-17}$$

where

$$A = \frac{G_{n+1} - G_n}{x_{n+1} - x_n} , \tag{A-18}$$

$$B = 2G_n , \tag{A-19}$$

and

$$C = 2\left(W_n - q\chi_0\right) . \tag{A-20}$$

This result is only useful if $A \neq 0$. Otherwise G is approximately constant in the neighborhood of x_n and a simpler procedure is possible. In this case,

$$\int_{x_n}^{x(q)} G(x)dx = G(x_n)\left[x(q) - x_n\right] , \tag{A-21}$$

and

$$x(q) = x_n + \frac{1}{G(x_n)}\left(q\chi_0 - W_n\right) . \tag{A-22}$$

Once a new gridding of the concentration profile is obtained, it may be necessary to refine the gridding by iteration. The transient transport equations are solved on the new grid, but without taking a new time step. With the newly obtained solution, the grid is re-calculated, and this process is repeated until the grid becomes stable.

The disadvantage of any adaptive gridding scheme is the necessity to interpolate the solution from one time step to the next resulting from the changing grid. As a consequence, if the spatial separation of grid points becomes too large, mass will no longer be conserved in spite of the mass conserving property of the finite difference scheme. Therefore, it is essential that over the region in which the solution is changing, the grid spacing be kept sufficiently small to ensure that interpolation errors are kept to a minimum.

A.2 REFERENCES

Press, W.H., B.P. Flannery, S.A. Terkolsky, and W.T. Vetterling. 1987. *Numerical Recipes.* Cambridge University Press.

NRC FORM 335 (2-89) NRCM 1102, 3201, 3202

U.S. NUCLEAR REGULATORY COMMISSION

BIBLIOGRAPHIC DATA SHEET

(See instructions on the reverse)

1. REPORT NUMBER (Assigned by NRC, Add Vol., Supp., Rev., and Addendum Numbers, if any.)
NUREG/CR-6347
CNWRA 94-018

2. TITLE AND SUBTITLE
Multi-Phase Reactive Transport Theory

3. DATE REPORT PUBLISHED
MONTH: July
YEAR: 1995

4. FIN OR GRANT NUMBER
B6666

5. AUTHOR(S)
P.C. Lichtner

6. TYPE OF REPORT

7. PERIOD COVERED *(Inclusive Dates)*

8. PERFORMING ORGANIZATION – NAME AND ADDRESS *(If NRC, provide Division, Office or Region, U.S. Nuclear Regulatory Commission, and mailing address; if contractor, provide name and mailing address.)*
Southwest Research Institute
Center for Nuclear Waste Regulatory Analyses
6220 Culebra Road
San Antonio, TX 78228-0510

9. SPONSORING ORGANIZATION – NAME AND ADDRESS *(If NRC, type "Same as above"; if contractor, provide NRC Division, Office or Region, U.S. Nuclear Regulatory Commission, and mailing address.)*
Division of Regulatory Applications
Office of Nuclear Regulatory Research
U.S. Nuclear Regulatory Commission
Washington, DC 20555-0001

10. SUPPLEMENTARY NOTES

11. ABSTRACT *(200 words or less)*

Physicochemical processes in the near-field region of a high-level waste repository may involve a diverse set of phenomena including flow of liquid and gas, gaseous diffusion, and chemical reaction of the host rock with aqueous solutions at elevated temperatures. This report develops some of the formalism for describing simultaneous multicomponent solute and heat transport in a two-phase system for partially saturated porous media. Diffusion of gaseous species is described using the Dusty Gas Model which provides for simultaneous Knudsen and Fickian diffusion in addition to Darcy flow. A new form of the Dusty Gas Model equations is derived for binary diffusion which separates the total diffusive flux into segregative and nonsegregative components. Migration of a wetting front is analyzed using the quasi-stationary state approximation to the Richards' equation. Heat-pipe phenomena are investigated for both gravity- and capillary-driven reflux of liquid water. An expression for the burnout permeability is derived for a gravity-driven heat-pipe. Finally an estimate is given for the change in porosity and permeability due to mineral dissolution which could occur in the region of condensate formation in a heat-pipe.

12. KEY WORDS/DESCRIPTORS *(List words or phrases that will assist researchers in locating the report.)*
heat and mass transport, partially saturated porous medium, Richards' equation, heat pipe phenomena, Dusty Gas Model, reactive transport, near-field

13. AVAILABILITY STATEMENT
unlimited

14. SECURITY CLASSIFICATION
(This Page)
unclassified
(This Report)
unclassified

15. NUMBER OF PAGES

16. PRICE